AN ABSTRACT OF THE THESIS OF

Megan J. Kaufman for the degree of Master of Science in Microbiology presented on November 15, 2011.

Title: Construction of a Model Organism for Performing Calcium Carbonate Precipitation in a Porous Media Reactor

Abstract approved:

_____

Frederick S. Colwell

Aquifers are an important storage location and source of fresh groundwater. They may become polluted by a number of contaminants including mobile divalent radionuclides such as strontium-90 which is a byproduct of uranium fission. A method for remediating such divalent radionuclides is sequestration through co-precipitation into calcium carbonate. Calcium carbonate precipitation occurs naturally but can be enhanced by the use of ureolytic microorganisms living within the aquifer. The microbial enzyme urease cleaves ammonia from urea (added as a stimulant to the aquifer) increasing the pH and subsequently pushing the bicarbonate equilibrium towards precipitation.

Laboratory experimentation is necessary to better predict field scale outcomes of remediation that is driven by ureolytic calcium carbonate co-precipitation. To aid in such laboratory experiments, I constructed two ureolytic organisms which contain green fluorescent protein (GFP) so that the location of the microbes in relation to media flow

paths and precipitation can be viewed by microscopy in a 2- dimensional porous medium flow cell reactor. The reactor was operated with a parallel flow regime where the two influent media would not promote microbially induced calcium carbonate precipitation until they were mixed in the flow cell.

A demonstration study compared the results of parallel flow and mixing in the reactor operated with and without one of the GFP-containing ureolytic organisms. The growth and precipitation of calcium carbonate within the reactor pore space altered flow paths to promote a wider mixing zone and a more widely distributed overall calcium carbonate precipitation pattern. This study will allow optimization of remediation efforts of contaminants such as strontium-90 in aquifers.

Construction of a Model Organism for Performing Calcium Carbonate Precipitation in a Porous Media Reactor

by

Megan J. Kaufman

A THESIS

Submitted to

Oregon State University

in partial fulfillment of

the requirements for the

degree of

Master of Science

Presented November 15, 2011

Commencement June 2012

Master of Science thesis of Megan J. Kaufman presented on November 15, 2011.

APPROVED:

_____

Major Professor, representing Microbiology

_____

Chair of the Department of Microbiology

_____

Dean of the Graduate School

I understand that my thesis will become part of the permanent collection of Oregon State University libraries. My signature below authorizes release of my thesis to any reader upon request.

_____

Megan J. Kaufman, Author

ACKNOWLEDGEMENTS

Funding for this work is from the DOE Office of Science. This thesis was possible because of the guidance and help of many people. My committee, especially my advisor Rick Colwell and his colleagues Robin Gerlach, Martin Schuster and George Redden were especially key in technical advising and support. I would like to thank my fellow lab mates Brandon Briggs and Heather Lavalleur for suggestions and support throughout my entire time here at OSU. I owe special thanks also to Adie Phillips, James Connolly, and Ellen Lauchnor who offered insight and training on the flow cell operation and organism construction. I would like to additionally thank Ellen for running our urea sample analysis. My sincerest gratitude also goes to Rashmi Gupta who was invaluable in the construction of the ureolytic clones. Michael Franklin also helped in early organism construction attempts. I am additionally indebted to Jason Balderston and Patrick Kaufman for consultation and for help in construction of the flow cells and cart. Thanks also to Adam Higgins along with Allyson Fry and Ratih Lusianti for use of and training on their fluorescent microscope, to Deborah Hobbs for use of a plate reader, and to Andy Ungerer for use and training on the ICP. I am also grateful to Chris Neighbor for his assistance in determining kinetic rates of ureolysis for my organisms. There are many others in Microbiology and COAS who deserve thanks. Last but not least I would also like to thank my family and friends for their continuing support.

TABLE OF CONTENTS

TABLE OF CONTENTS (Continued)

LIST OF FIGURES

LIST OF FIGURES (continued)

LIST OF TABLES

Construction of a model organism for performing calcium carbonate precipitation in a porous media reactor

Introduction

An aquifer is a geological formation that contains sufficient saturated, permeable material to yield significant quantities of water to wells and springs (USGS "Groundwater Information"). As well as being important in ecological systems such as wetlands, they are relied heavily upon for drinking water, irrigation, industry and livestock (US EPA "Groundwater"). An aquifer may become unfit for drinking through a number of ways including through salt-water intrusion or from arsenic being dissolved from natural sources. Land use can also cause the water to become unsafe for consumption through the accumulation of pesticides or herbicides, nitrates from fertilizers, organics or pathogens from livestock or human waste, or from leaking underground storage tanks or landfills (US EPA "Groundwater"). Mining operations or careless disposal of nuclear waste may introduce heavy metals or radionuclides (US EPA "Groundwater").

After contamination of an aquifer occurs, a decision must be made as to the best course of action. In certain cases, such as with nitrite contamination from fertilizers, the aquifer often must be retired from use or simply monitored as cleaning is not feasible (Alabama Department of Environmental Management "Groundwater Contamination"). In other cases, remediation of the aquifer may be possible. Different types of

remediation exist depending on the type of contaminant and situation. Some examples include excavation of contaminated soils or so called ‘pump and treat’ of water where wells are drilled based on location of the contaminant plume and water is pumped to the surface, treated and returned to the aquifer(US EPA "Basics of pump and treat groundwater remediation technology"). A different kind of remediation is bioremediation. This technique exploits the abilities of microorganisms to degrade or immobilize harmful compounds and can be used either *in situ* or *ex situ*, through the addition of microbes, nutrients, electron donors or electron acceptors (US EPA "Use of bioremdiation at superfund sites").

Currently the approach used to clean up sites contaminated with divalent radionuclides such as strontium-90 (Sr-90) is an expensive pump and treat approach (Fujita et al. 2008). An alternative approach is the long term sequestration of the radionuclide by co-precipitation into calcium carbonate within the aquifer. Calcium carbonate precipitation occurs naturally at slow rates within aquifers but can be enhanced by increasing the alkalinity and pH of the system. One way to increase the alkalinity and pH of an aquifer is to encourage microbial breakdown of urea (ureolysis). Microbial communities in the aquifer respond to urea by production of urease, an enzyme that cleaves ammonia from urea and thereby shifts the bicarbonate equilibrium towards precipitation of carbonates, incorporating calcium or strontium. If, through co-precipitation remediation, the divalent radionuclide substitutes into the calcium

carbonate lattice and becomes immobilized the risk to downstream populations who use the aquifer water can be minimized (Fujita et al. 2000).

One problem encountered with the method that involves co-precipitation of contaminants into calcium carbonate for radionuclide remediation is in the control of the reaction. In an early field test the site of injection became plugged by calcium carbonates (Fujita et al. 2008). Others have also witnessed the majority of calcium carbonate being deposited near the injection wells as in a large scale sandbox study investigating biogrouting as a soil improvement method (van Paassen et al. 2010). Similarly, immediate precipitation of calcium carbonate from supersaturated fluids flowing through artificial fractures was observed near the inlet of an injection, preventing any further 'downstream' precipitation (Emmanuel and Berkowitz 2005). By simulating the process of microbially mediated calcium carbonate precipitation in laboratory model flow cells, insight may be gained into the interaction of the precipitation, flow paths and organism distribution.

A laboratory environment can offer advantages for modeling and learning more about a process. Model organisms may be custom-engineered for use in laboratory studies without ever having the intention of using them in the environment being simulated. For example, laboratory organisms are often engineered to contain a green fluorescent protein (GFP). The protein was isolated from the jellyfish *Aequorea victoria* (Larrainzar, O'Gara, and Morrissey 2005). Enhanced variants of the protein

autofluoresce green (530 nm) upon stimulation by a wavelength of light near 485 nm (Werner et al. 2004). The GFP may be linked to a specific activity of the cell, for instance to the transcription of a protein of interest. This fluorescence can be seen as green in a microscope with the correct filter without the addition of any other substances and without killing the cells. In laboratory flow cells, this allows for visualization of the microorganisms during experiments without destructively staining them.

The overall objective of my research was to develop strategies that could help optimize calcium carbonate precipitation distribution within a porous medium. My goals were to: (1) develop a better tool for visually examining calcium carbonate precipitation being mediated by microbes in porous media, and (2) demonstrate the effectiveness of using that tool within a flow cell model system. To address the first goal I constructed two ureolytic, GFP containing microorganisms that could be visualized within a flow cell undergoing ureolysis and subsequent calcium carbonate precipitation. To address the second goal I used a parallel flow strategy in a 2D porous media flow cell where complementary solutions came into contact through mixing. In this mixing zone of the media the ureolytic organisms would be able to precipitate calcium carbonate. I hypothesized that the growth of ureolytic microorganisms and resulting calcium carbonate precipitation would create a wider mixing zone by disruption of the bulk flow direction and introduction of transverse flow paths. I used a two dimensional porous media flow cell system that was transparent to microscopic and macroscopic imaging to observe the resulting mixing patterns, localization of cells and precipitation at a pore

scale level. Both the construction of ureolytic GFP organisms and the investigation of parallel flow mixing zones are first steps towards understanding and predicting outcomes of larger, field-scale remediation efforts.

Literature Review

Aquifers

Aquifers are important for life on earth as they are a storage and supply reservoir for fresh groundwater. Figure 2.1 gives an impression for how much fresh water can be hidden from view below the surface of the earth. Groundwater is so important because of all the water on the planet, only 1% is fresh water and 99% of that supply is groundwater (USGS "Groundwater Information"). The United States pumped an estimated 79.6 billion gal/day of fresh groundwater in 2005 (USGS "Groundwater Information"). This water was used for drinking water, irrigation, industry and livestock (US EPA "Groundwater"). Aquifers may become polluted by contaminants and while prevention of contamination is always preferred, once contamination has occurred remediation may be necessary.

If remediation of an aquifer is aided in some way through the actions of microorganisms it is considered bioremediation (Griebler and Lueders 2009). Certain contaminants can be degraded directly by microorganisms, if the correct conditions and organisms are present. For example, petroleum hydrocarbons, aromatic hydrocarbons such as volatile organic compounds from landfill leachates, halogenated hydrocarbons, and even some pesticide residues can be broken down by microbial enzymes (Wallrabenstein et al. 1995; Rahm et al. 2006; Roling et al. 2001; de Lipthay et al. 2002). In the case of some radioactive metals, such as uranium, certain organisms can reduce

the soluble U(VI) form to an insoluble U(IV) form (Holmes et al. 2002). Other metals such as lead, zinc and cadmium along with divalent radionuclides such as strontium-90 or cobalt-60 can be immobilized through co-precipitation into surrounding calcium carbonates (Fujita et al. 2000). In these cases the precipitation of calcium carbonate can be enhanced by the presence and activity of microorganisms.

The subsurface environment

The subsurface consists of sediments or rocks with pore spaces and fractures of various sizes. The pores may contain water and/or air. Flow and exchange of water occurs between the aquifer and surface systems, but, the rates of exchange can vary widely (Figure 2.1). Residence times in aquifers can vary from 2 weeks to 100,000,000 years (Griebler and Lueders 2009). Dissolution and precipitation reactions between the fluid water and the surrounding matrix result in a physico-chemistry affecting the overall geochemistry including pH, ionic strength and solution composition (Saripalli et al. 2001). Together all of these physical and chemical factors determine the nature of the habitat for biological organisms and subsurface life.

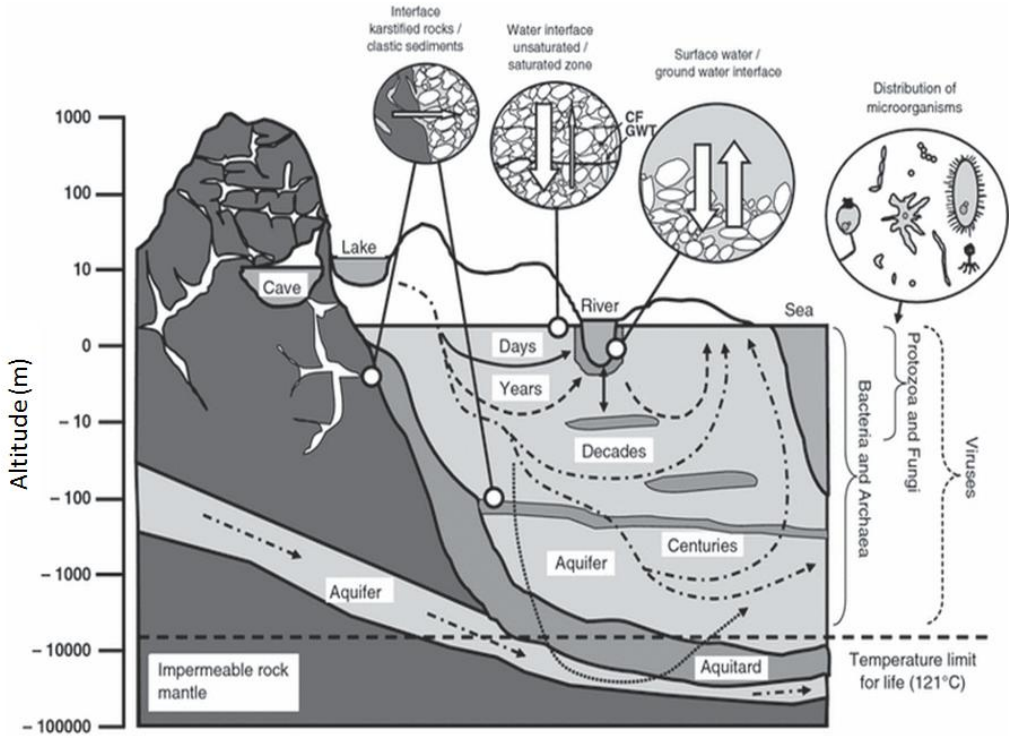

Figure 2.1. Schematic view of aquatic surface and subsurface habitats. Arrows depict the flow of water carrying energy and matter through the subsurface, with boxes next to arrows indicating typical groundwater residence times. Circles highlight transition zones between habitat types. Curly braces indicate the distribution of different microbial groups in the subsurface. CF, capillary fringe; GWT, groundwater table. Figure from Griebler and Lueders 2009 (Reprinted with permission license number 2765521498584).

Aquifer sediments, grains, pore-water, spaces, and rock and fissure water all create habitat for microorganisms. It has been estimated that up to 40% of the planet's prokaryotic biomass is hidden within the subsurface of the earth (Whitman, Coleman, and Wiebe 1998). This can amount to up to 22-215x10^{12} kg of biomass (Griebler and Lueders 2009). This subsurface prokaryotic life consists mainly of bacteria and archaea but also protozoa and fungi (Griebler and Lueders 2009). The organisms found are

mostly heterotrophs well adapted to low levels of nutrients available in the aquifer environment or lithoautotrophs that oxidize inorganic electron donors (Ghiorse and Wilson 1988; Stevens and McKinley 1995). Functional groups of the microorganisms found can include methane and ammonia oxidizers, denitrifiers, sulfate reducers or methanogenic archaea (Griebler and Lueders 2009).

Factors controlling the spatial distribution of microorganisms within aquifers are spatial heterogeneity, temporal variability, and disturbances (such as the addition of pollution/stimulants) (Griebler and Lueders 2009). Most aquifer microorganisms are believed to be attached to sediment rather than free-living (Griebler and Lueders 2009), but that ratio has also been found to depend on the levels of dissolved organic carbon and nutrients available, as well as on mineralogy and sediment size (Bengtsson 1989) Microorganisms growing attached to sediment or other surfaces (rather than being free-floating or planktonic) are referred to as biofilm (Davey and O'Toole 2000). The biofilm consists of the microorganisms themselves, but also of substances excreted by the cells. For example, exopolysaccharides (EPS) are commonly found in association with biofilm and are believed to help hold the communities together (Southey-Pillig, Davies, and Sauer 2005; Stapper et al. 2004).

While the environment affects biofilm growth through hydrologic factors including groundwater flow velocity, residence time and hydraulic gradient, the biofilm growth in porous media in turn affects the hydrodynamics and flow paths. Whether

through physical impedance or through chemically altering their surrounding environment, the presence of the microorganisms results in a changed biogeochemistry of the subsurface environment. Both the dense physical structure of biofilm material as well as the metabolism of the microbes themselves affect hydrodynamic properties in the subsurface such as porosity, permeability, pore and particle size distributions (Saripalli et al. 2001). Biofilms can impact these parameters so greatly that much research has gone into engineering biofilm barriers. Biofilm barriers can be used in subsurface remediation, enhanced oil recovery, abatement of saltwater intrusion, filtration, deep subsurface sequestration of supercritical carbon dioxide and biofouling of injection or recovery wells (Cunningham et al. 2003; Dutta et al. 2005).

Fluid mixing in the subsurface

Understanding the factors (abiotic or biotic) that will influence hydrodynamic pathways becomes especially important when we want to predict or control the movement of fluids under the surface of the earth. For instance, when an aquifer becomes contaminated we want to know when and where the substance will migrate. Mathematical models, laboratory scale models, or a combination of the two, are useful in studying reactive transport in porous media because it cannot be observed directly in the field (Gramling, Harvey, and Meigs 2002). Flow cell models of porous media simulating an aquifer are often operated to provide a convenient experimental scale that can be controlled with respect to various factors. However, in order to predict the

outcome of large, field-scale results of pumping two reactive solutions together, we first must understand the underlying pore scale interactions. When 'scaling up' from pore (mm) to Darcy (dm or cm) to field-scales (m), prediction of outcomes is not linear (Acharya et al. 2007). This is evident from a number of papers (some of which are summarized below) concerning mixing within porous media.

Mixing occurs when two or more fluids come together. This can create disequilibrium resulting in chemical reactions (De Simoni et al. 2007). For instance, where a contaminant plume travels into fresh groundwater, reactions occur along the leading edges or fringes of the plume (Werth, Cirpka, and Grathwohl 2006). A coefficient for modeling the mixing process is called 'hydrodynamic dispersion' and describes the spread of solutes about an advective front. It can be experimentally determined by adding a tracer to the fluid. At normal groundwater flow rates in homogeneous porous media, this coefficient will be determined primarily by mechanical dispersion. However, at a pore-scale the concentration of the tracer may be determined more by molecular diffusion and may be highly variable resulting in a different calculation of the dispersion coefficient (Gramling, Harvey, and Meigs 2002). In essence, a multiple pore-space averaged estimate will over-estimate the amount of reaction occurring because of the assumption of pore-scale mixing. Acharya et al. (2007) also found that dispersion coefficients measured through tracer spreading cannot be applied to model mixing in reactive transport, especially for up-scaling from pore to Darcy scale. Tartakovsky and Redden found large concentration gradients of solutions in modeling pore-scale

simulations of mixing reactions that do not agree with Darcy-scale advection-dispersion equations (Tartakovsky and Redden 2008). In another example that considered heterogeneous breakthrough curves at single points versus over an integrated control plane, it was found that the effective dispersion coefficient is about 2/3 of the macrodispersion coefficient (Jose, Rahman, and Cirpka 2004). Jose, Rahman and Cirpka found instead that mixing and spreading are equivalent after a characteristic pore-scale dispersion time where transverse rather than longitudinal dispersion is most critical for determining overall extent of plumes in persistent contaminant sources. Assumptions of homogeneity in porous media are problematic and such assumptions can explain why field-scale dispersivities are often larger than laboratory derived ones (Werth, Cirpka, and Grathwohl 2006). For example, transverse dispersion across adjacent streamlines can control rates of mixing. When groundwater flow converges into a high-permeability zone (around low permeability ones) the distance required for a solute to cross a given number of streamlines decreases. This enhances transverse mixing and reaction rates (Werth, Cirpka, and Grathwohl 2006).

While mixing within porous media takes place on a small, pore-scale level it will ultimately determine the field-scale results. In the case of microbially enhanced mixing resulting in calcium carbonate precipitation, we need to understand more about the pore scale reactions taking place. Specifically, we need to better understand the interactions between the microbes driving the reactions, the fluid flow paths, and precipitation patterns. These interactions would be elucidated by a better way to

visualize the location of the microbes in relationship to the calcium carbonate and flow paths during an experimental trial.

Calcium carbonate precipitation

Calcium carbonate reactions can be of anthropogenic benefit when controlled in a variety of applications. Prevention of the reaction is beneficial in the medical field where uropathogenic strains of bacteria can cause infection (Mobley and Hausinger 1989). It is also important in agriculture and the effective application of fertilizers. Here, maximum benefit is achieved if the urea added to fields is hydrolyzed at a controlled rate for slow release to the crop as ammonia (Boquet, Boronat, and Ramos-Cormenzana 1973). The enhanced precipitation of calcium carbonates is of interest in efforts to strengthen soil for land use applications (Whiffin, van Paassen, and Harkes 2007), statue repair (Ciferri 1999), oil recovery (Ferris et al. 1996), dust control (Meyer et al. 2011), and self-healing cement (Bang, Galinat, and Ramakrishnan 2001). An emerging focus of enhanced precipitation of calcium carbonate is to aid in the remediation of certain divalent metal or radionuclide contaminants in aquifers (Fujita et al. 2000). This remediation application (described below) is the system used as a model for studying mixing wherein the control of mixing reactive solutions is used to increase calcium carbonate precipitation throughout a simulated porous medium using ureolytic microorganisms.

The precipitation of calcium carbonate is a process that occurs naturally and continually within the environment (Boquet, Boronat, and Ramos-Cormenzana 1973; Hammes and Versraete 2002). Precipitation of calcium carbonates in the environment may be abiotic in nature and controlled mainly by pressure, temperature, and hydrodynamic conditions such as fluid flow (Saripalli et al. 2001) or it may be mediated by microorganisms living in the subsurface environment (Tobin et al. 2000). The presence of microbes may facilitate the precipitation by acting as a heterogeneous nucleation point upon which the precipitation may occur (reducing the energy of activation of the reaction) as well as through their metabolic activities altering the chemical environment (Banfield and Nealson 1997). For instance, an increase in pH can alter the bicarbonate equilibrium toward precipitation if calcium is present in high enough concentrations.

Urease to promote calcium carbonate precipitation

Calcium carbonate precipitation is largely dependent on solution pH. One way that an organism can alter the environmental pH surrounding it is through a process called ureolysis. Organisms that can perform this function contain an enzyme, urease, which cleaves ammonia from urea. There are both eukaryotic and prokaryotic ureases found in a variety of organisms including yeasts, filamentous fungi, bacteria, algae and plants (c.f. (Mobley and Hausinger 1989) and references therein). The enzyme is often cytoplasmic in bacteria and yeasts, although some species host periplasmic or

extracellular urease (Mobley and Hausinger 1989). Control of the enzyme may be constitutive, inducible or repressible depending on the organism (Mobley and Hausinger 1989). The overall structure is known to vary in the number of subunits (between 1 to 3) and the number of each subunit needed to complete the protein (between 3 to 6). However, in all known ureases, the active site of the enzyme contains two nickel ions. Thus, the presence and concentration of nickel can control the performance of the urease in the medium (Mobley 1995).

The chemical changes brought about by the activity of urease in a calcium containing aqueous environment have been well described. During the ureolysis reaction ammonia hydrolyzed from urea undergoes a reaction with water to form ammonium ions and produces carbonate in the process. The resulting changes in chemistry cause a precipitation of calcium carbonate as described in the following equation (van Paassen et al. 2010):

1) $H_2NCONH_2 + 2H_2O \leftarrow_{urease} \rightarrow 2NH^{4+} + CO_3^{2-}$

2) $Ca^{2+} + CO_3^{2-} \rightarrow CaCO_3$ (s)

This process in an aquifer contaminated with trace metals such as lead, zinc, cadmium or radionuclides such as Sr-90 or Co-60 will cause co-precipitation of the contaminant along with the calcium (Fujita et al. 2000). Figure 2.3 shows an example using Sr-90. The urease enzyme cleaves ammonia from urea. The rise in ammonia levels promotes desorption of calcium and strontium (if present) from the aquifer walls and

the high pH and carbonate concentrations will precipitate calcium (or strontium) carbonates. The divalent structure of Sr-90 will cause it to substitute into the crystal lattice of the carbonate in place of (and in addition to) calcium. The Sr-90 will then remain sequestered in the minerals of the aquifer-bearing geological unit.

An advantage to using microbial urease to enhance the rates at which this reaction occurs over simply injecting a base to change the pH of the system is that the microorganisms allow for a delay in the precipitation reaction. This is important when trying to optimize the reaction to occur throughout the aquifer rather than mainly occurring at the injection site.

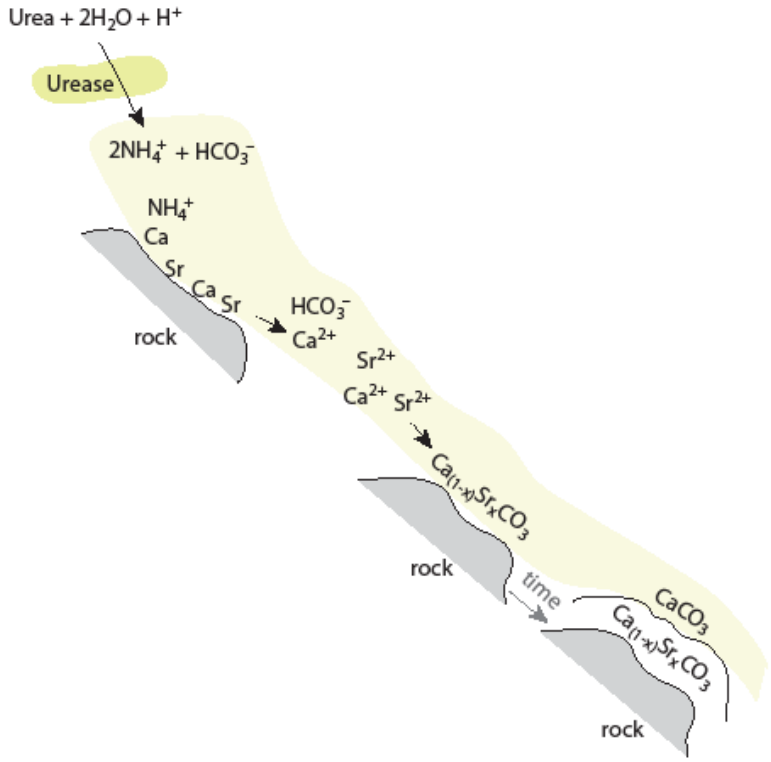

Figure 2.2. Representation of ureolytically driven calcium carbonate precipitation within an aquifer. Urease hydrolyzes urea to produce NH_4^+, HCO_3^- and raises pH. HCO_3^- interacts with Ca^{2+} to form $CaCO_3$ precipitation. Continued precipitation causes changes in flow paths. Modified from Colwell et al. (2005).

Problems have occurred when implementing *in situ* co-precipitation into calcium carbonate remediation strategies. A pilot project aimed at enhancing the rates of microbial precipitation of calcite was performed at a test aquifer. By injecting ureolysis stimulating materials (molasses and urea) the experiment resulted in the plugging of the well. In the area immediately adjacent to the well levels of bacterial urease were found to have increased suggesting that the precipitation front was at least partially due to the

activity of the naturally occurring microbes (Fujita et al. 2008). The authors concluded that the reaction had occurred too quickly immediately surrounding the well for the stimulating material to penetrate deep into the aquifer. Likewise, other studies investigating mineralization of supersaturated fluids of calcium and carbonates reported most of the deposition occurring within several centimeters of an inlet or even clogging the inlet completely (Lee and Morse 1999; Hilgers and Urai 2002; Fujita et al. 2008). These studies underscore the need to better understand how the mixing of the reactants can be accomplished to better control the precipitation rates and distribution patterns of the mineral.

Research into how to control the precipitation of calcite often enlists the help of microbes that are capable of enhancing the rates at which it occurs. These microbes may be native assemblages or populations in an aquifer or in some cases an organism may be added to the system (van Paassen 2010). As previously mentioned *in situ ureC* gene levels within an aquifer increased measurably after treatments of molasses and urea were amended to the groundwater (Fujita et al. 2008). Furthermore, samples of groundwater that were amended with molasses in a flask study and subsequently tested for urea hydrolysis showed high levels of activity (Colwell et al. 2005). An effort to isolate native ureolytic bacteria from an aquifer in Idaho revealed the presence of multiple ureolytic organisms and further analysis of 16s rRNA gene sequences in a subset of the population indicated the presence of *Pseudomonas spp.* and *Variovorax spp*. (Fujita et al. 2000).

Other than using native communities *in situ* for calcium carbonate experiments, some organisms have been either isolated and cultivated or genetically constructed for use in laboratory simulation studies. Listed below are candidate microorganisms that can be considered as models for flow cell experiments involving calcium carbonate precipitation.

Model ureolytic microorganisms

The most prevalent organism in the calcium carbonate literature, *Sporosarcina pasteurii* (previously *Bacillus pasteurii* (Yoon et al. 2001)) is often used in microbially amended calcium carbonate precipitation work (Whiffin, van Paassen, and Harkes 2007; Ferris et al. 2004; Stoner et al. 2005). It is a soil organism that is naturally constitutively ureolytic (Mobley 1995). Uptake of ammonium across the cell membrane is passive and therefore growth of the organism requires high levels of ammonia and high pH (Morsdorf and Kaltwasser 1989). Its rates of ureolysis are very high and its specific enzyme activity can reach 16,900 mU/mg protein (Morsdorf and Kaltwasser 1989). However, a drawback to using this organism for certain laboratory applications is that it is difficult to transform genetically (J. Henriksen, personal communication). This makes it a poor candidate for genetic manipulation such as the addition of a GFP.

Pseudomonas aeruginosa has a large and metabolically diverse genome. Perhaps because of this it is ubiquitous in the environment and is often isolated from soils and waters (Stover et al. 2000). Strain PA02175 has been shown to possess urease and to

perform ureolysis under certain conditions in which nitrogen is limiting at levels of about 1,600 mU/mg protein (Janssen et al. 1982; Janssen 1981). (Note that this activity occurs at a level 10-fold lower than *S. pasteurii)*. This places it in the category of urease being under repressible control. Control of the urease operon appears to be associated with glutamine synthetase (Janssen et al. 1982). Partly due to the medical interest in the organism, much work has been done on transforming the cells and GFP strains exist (e.g. Werner et al. 2004).

Bacillus subtilis 168 possesses a UreABC operon (Cruz-Ramos 1997) and is found to increase urease synthesis for many strains in nitrogen-poor media by up to 25 fold for enzyme specific activity rates approaching 205 U/mg protein (Atkinson and Fisher 1991). (This value and/or unit seem to be high but are as reported.) It is a known soil organism and forms biofilms (Hamon 2004; Kearns 2005). Significantly, as a model organism, its stress response is well understood and several key genes can be linked to stress experienced by the cells (Gruber and Gross 2003). This could mean that its physiological health could potentially be tracked during lab studies if a shortened half-life GFP construct was used.

Microorganisms may be genetically constructed to contain genes for certain phenotypic traits as desired in order to conduct experiments. The urease operon has been cloned into non-ureolytic organisms (Zhang et al. 2009; Collins and Falkow 1990). In the case of *E. coli* DH5α(pURE14.8), an isolated DNA sequence containing the urease

genes was introduced to *E. coli* DH5α for expression. This DNA was introduced by means of a plasmid (pUC19) that was constitutive to express the urease genes (Collins and Falkow 1990). With further genetic manipulation, these urease genes could be cloned into a previously constructed GFP organism. The resulting GFP organism would then also be ureolytic, or able to carry out calcium carbonate precipitation in a porous medium.

To address the issues noted above, the objective of this work was to construct a GFP containing, ureolytic microorganism to be used in a laboratory scale flow cell reactor. The reactor simulates an aquifer undergoing remediation by microbially enhanced calcite precipitation. The addition of two complimentary media, in a parallel flow would provide the organism with materials for calcium carbonate precipitation only in the mixing zone. The GFP would allow for visualizing the location of the microbe within the flow cell at a microscopic scale. This information could be incorporated with macro scale observations of resulting flow paths (Figure 2.3).

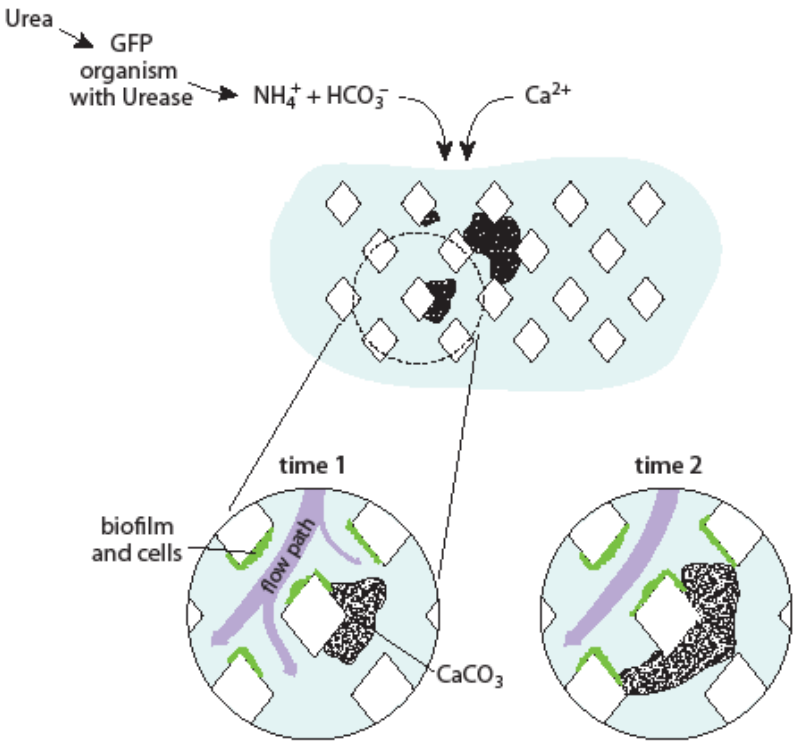

Figure 2.3. Representation of ureolytically driven calcium carbonate precipitation within a simulated porous media flow cell system. The urease in the constructed GFP organism hydrolyzed urea to produce NH_4^+, HCO_3^- and raises pH. HCO_3^- interacts with Ca^{2+} to form $CaCO_3$ precipitation. Continued precipitation causes changes in flow paths.

Summary

Aquifers are an invaluable resource for clean, potable water and the protection of them is a priority. In case contamination occurs, the remediation method becomes an important consideration. Using knowledge of how subsurface microorganisms can alter the biogeochemical environment of an aquifer we can promote processes that aid in remediation efforts. For example, microbially mediated calcium carbonate precipitation has been investigated as a method to sequester the normally mobile Sr-90 (a toxic divalent radionuclide) to the minerals in the aquifer. Despite the promise of this approach difficulties remain. A greater understanding of pore scale behavior is required to be able to predict and control the process at a field scale. By modeling different mixing regimes in a laboratory scale flow cell model, it is possible that we can learn how the organisms, the flow paths and the resulting precipitation patterns are connected. The use of model microbes that hydrolyze urea is useful in such studies. This would be aided by the creation of a ureolytic organism containing GFP that would allow for visualization of the microorganism within the flow cell while the process is being carried out.

Materials and Methods

Bacterial strains and growth conditions

Overnight broths of the organisms used in this work were grown as indicated in Table 3.1. All were grown with shaking at 200 rpm at 37 ^{o}C except *S. pasteurii* which was grown at 30 ^{o}C.

Table 3.1. Bacterial strains and media used in this work.

Strain	Relevant properties	Growth media	Source	Reference
Pseudomonas aeruginosa AH298	GFP on chromosome	Luria-Bertani (LB) (MoBio Laboratories)	R. Gerlach	Werner et al. 2004
Pseudomonas aeruginosa MJK1	AH298 with urease added on pJN105 plasmid	LB plus 100 µg/ml gentamicin (Sigma)	This work	NA
Escherichia coli DH5α(pURE14.8)	Urease operon on pUC19 plasmid	LB plus 50 µg/ml ampicillin (Sigma)	J. Henriksen	Collins and Falkow 1990
Escherichia coli AF504*gfp*	GFP on chromosome	LB plus 100 µg/ml ampicillin	A. Folkesson	Folkesson et al. 2008
Escherichia coli MJK2	AF504*gfp* with urease added on pJN105 plasmid	LB plus 10 µg/ml gentamicin	This work	NA
Sporosarcina pasteurii	Urease constitutive organism	Brain Heart Infusion (BHI) (Fluka) plus 2% urea (Mallinckrodt Chemicals)	J. Henriksen	NA

All overnight cultures were collected by centrifugation at 2500 rcf and washed to remove spent media, resuspended in 500 µl of a modified calcite mineralizing media (CMM) (Ferris et al. 1996) (Table 3.2). These washed cultures were transferred into 30 ml CMM base complete for flask studies or into 4 ml CMM base with calcium or with urea for flow cell inoculations, each with the appropriate antibiotic, and 50 mM L-arabinose (Sigma).

Table 3.2. Formulae for different variations of CMM used in experiments. The original CMM is described in Ferris et al. 1996.

Medium	Standard Nutrient broth No. 1 (Sigma) (g/L)	Sodium bicarbonate (M. Chem.) (g/L)	Nickel (II) chloride hexa-hydrate (Sigma) (µM)	Urea (M. Chem.) (g/L)	Calcium chloride dihydrate (M. Chem.) (g/L)	Ammonium chloride (NA) (g/L)
CMM base w/calcium	3	2.1	10	----	3.7	-----
CMM base w/urea	3	2.1	10	20	----	-----
CMM base complete	3	2.1	10	20	3.7	-----
CMM base complete w/o nickel	3	2.1	-----	20	3.7	-----
CMM (Ferris et al. 1996)	3	2.1	-----	20	3.7	10

(1 -M.Chem. = Mallinckrodt Chemicals).

Plasmid and model organism construction

To construct *P. aeruginosa* MJK1 and *E. coli* MJK2 a previously constructed ureolytic strain *E.coli* DH5α(pURE14.8) was used (Collins and Falkow 1990). The pUC19 plasmid carrying the urease operon was extracted (Figure 3.1). The operon includes urease structural genes *ureABC* and putative accessory genes *ureD* and *ureFG* used to acquire nickel (Kim, Mulrooney, and Hausinger 2006). Polymerase chain reaction (PCR) primers (Eurofins Operon) were designed for either end of the insert with restriction sites *PstI* and *SpeI* added to the 5' end (Figure 3.1). Sequences of the primers that were used can be found in Appendix A. PCR amplification of the region was performed. Digestion with the appropriate restriction enzymes (*PstI* and *SpeI*, New England Biolabs) was completed before ligating (Invitrogen ligase) into a pre-digested pJN105 vector (Newman and Fuqua 1999) (Figure 3.1). This plasmid is inducible with L-arabinose (Newman and Fuqua 1999).

This ligation was used to transform *E. coli* cells (*max efficiency,* Invitrogen) and plated onto LB plates containing gentamicin (100 μg/ml). Suspected transformants were screened by electrophoretic gels loaded with restriction-digested plasmids extracted from each clone. Functional tests for ureolysis were performed in urea broth (Fluka) containing the appropriate antibiotic and L-arabinose (final concentration 50 mM).

The extracted pJN105 plasmid containing the urease operon was transformed into the cell strains AH298 and AF504*gfp* (Figure 3.1). Both of these strains already

contained an altered and unstable GFP variant (Werner et al. 2004; Folkesson et al. 2008). Both GFP variants contain an amino acid sequence at the C-terminal end that is recognized for degradation by proteases within the cell (Andersen et al. 1998). This causes the newly made GFP protein to have a short half-life resulting in the disappearance of signal over time unless new GFP is created to replace it (Sternberg et al. 1999).This altered GFP in AH298 is linked to the growth rate dependent ribosomal promoter *rrnBp*$_1$ (Werner et al. 2004). In this way a more accurate view of the metabolic activity levels of the cells can be achieved. The GFP in the *E. coli* strain AF504*gfp* was added to the chromosome and is constitutively produced (Folkesson et al. 2008).

Finally, the newly transformed GFP-expressing organisms were checked for urease functionality in urea broths containing L-arabinose at 50 mM and the appropriate antibiotic.

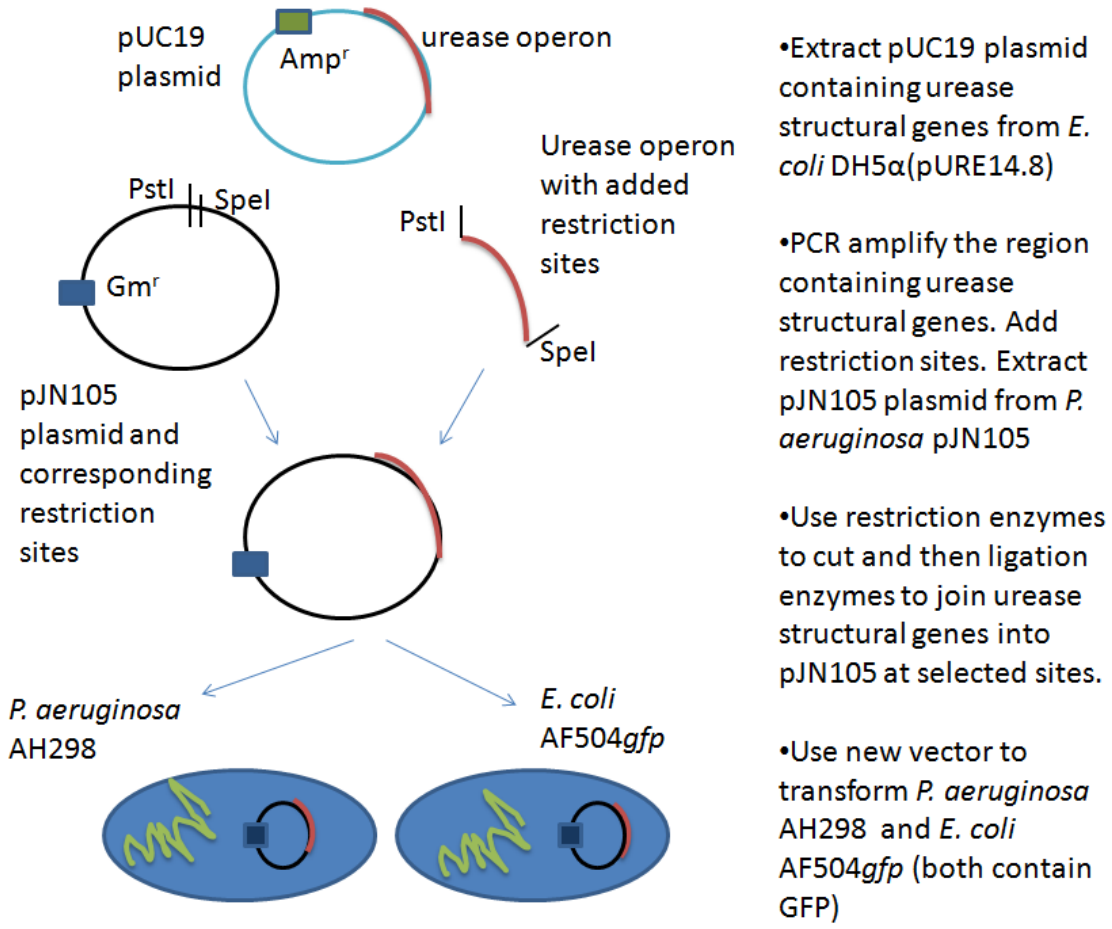

Figure 3.1. Overview of the cloning procedures undertaken to construct the GFP ureolytic organisms MJK2 and MJK1. Amp^r refers to an ampicillin resistance marker and Gm^r to a gentamicin resistance marker.

Urease gene sequencing

Sequencing of the ends of the transforming vector pJN105 and of the urease gene insert was done in a step-wise manner because the length of the inserted urease operon was longer than an individual sequencing run. First, primers (Eurofins operon

HPSF purified) for either side of the pJN105 insertion site were used to sequence partially into the insert. The sequence of these primers can be found in Appendix A. This new sequence information then allowed for the design of new primers at the ends of the newly sequenced section. Thus, for each of the newly sequenced sections, primers were designed until the sequencing eventually reached across the insert. The sequencing was conducted by the Center for Genome Research and Biocomputing at Oregon State University. Samples were run on an ABI Prism® 3730 Genetic Analyzer using ABI Prism® 3730 Data Collection Software v. 3.0 and ABI Prism® DNA Sequencing Analysis Software v. 5.2. Two base callers were used one called KB Basecaller (Applied Biosystems) and the second called base caller 3730pop7LR (Applied Biosystems).

Ureolytic batch studies

Flask studies were performed to ensure that the ureolytic organisms MJK1 and MJK2 would be able to promote calcium carbonate precipitation. DH5α(pURE14.8) and *S. pasteurii* were used as positive controls, and the non-transformed AH298 and AF504*gfp* as negative controls. The flask studies began by inoculating washed cells (as described earlier) into 30 ml of CMM base complete with or without nickel (Table 3.1) with appropriate antibiotic and 50 mM L-arabinose. Over 3 day incubation periods at room temperature and without shaking, flasks were sampled daily for pH, calcium, ammonium, urea and visual precipitation. Analyses were performed as described below.

Analytical measurements to monitor ureolysis

To determine calcium concentrations, samples were filtered (0.22 µm filter, sterile PVDF, Fisher Scientific) and stored at 20^{o}C until analysis. For analysis, samples were diluted to within calibration range (0-20 mg/L calcium) into 1% distilled nitric acid (Mallinckrodt Chemicals). Diluted samples were then analyzed on a Prodigy high dispersion inductively coupled plasma (ICP) instrument (Leeman Labs Inc.). Analysis was done using Salsa software (JMM). Calcium peaks were measured in radial view on line Ca 317.933r and compared to a calcium standard (Ultra Scientific). In order to estimate the amount of calcium precipitated in the reactor after the flow cell experiment was done, the flow cell was opened and 500 µl of 10% nitric acid was added to four different regions (quadrants near influent or effluent for either influent port) of the flow cell. The acid was recovered and filtered, then diluted and analyzed by ICP as described above.

A modified Nessler Method was used as described previously to measure ammonium (Whiffin, van Paassen, and Harkes 2007). Samples were similarly filtered and stored at 20^{o}C until analysis. Samples were diluted to between 0 to 20 ppm (mg/L). Diluted samples were pipetted (0.25 ml) to the wells of a 96 well plate. Polyvinyl alcohol dispersing agent (3 µl, Hach) and mineral stabilizer (3 µl, Hach) were added followed by Nessler reagent (10 µl, Aldrich) and the mixture measured after 13 minutes at 425 nm on a Molecular Devices SpectraMax 190 spectrophotometer using Softmax pro 5.2 software. The pH was measured using a bench top meter (VWR Symphony). Urea was

analyzed by a modified high performance liquid chromatography (HPLC) method (Clark et al. 2007) at Montana State University (MSU) after 0.22 µm filtration and dilution to within calibration range (5-200 mM urea). Samples were kept at 20^{o}C until being shipped on ice overnight. Chris Neighbor determined kinetic rates of ureolysis for each strain of organism (*S. pasteurii*, AH298, AF504*gfp*, MJK1 and MJK2) by measuring the rates of urea hydrolysis per cell over time in flask studies (C. Neighbor, personal communication).

Operation of the flow cell

The flow cell reactor was operated to evaluate the performance of the newly constructed ureolytic organism to both fluoresce and to precipitate calcium carbonate in a simulated porous medium, and to establish distribution patterns of the calcium carbonate under a parallel flow regime where the mixing of two media allowed for precipitation. The flow cell system for these experiments was designed and constructed at the Center for Biofilm Engineering at MSU. The flow cells were 12 cm x 18 cm, polycarbonate material with 1 mm etched pores over an area of 4 cm x 8 cm. Fluids were pumped through the flow cell using a peristaltic pump (Masterflex, model 7520-50) with 'Easy Load 2' heads. All tubing used was composed of silicone peroxide (Masterflex, 96400 size 13, 16 and 25). Flow rates were determined volumetrically and adjusted to a rate of 1.0 ml/min. Media used were CMM base with calcium in one inlet and CMM base with urea in the other (Table 3.1). When the two media mixed in the

flow cell, all the necessary components for calcium carbonate precipitation were present (CMM base complete). However, prior to mixing the respective influent solutions were independently incapable of promoting precipitation. L-arabinose (50 mM) and gentamicin (100 μg/ml) were added in order to induce the urease gene and to maintain the plasmid in the MJK2 cells respectively.

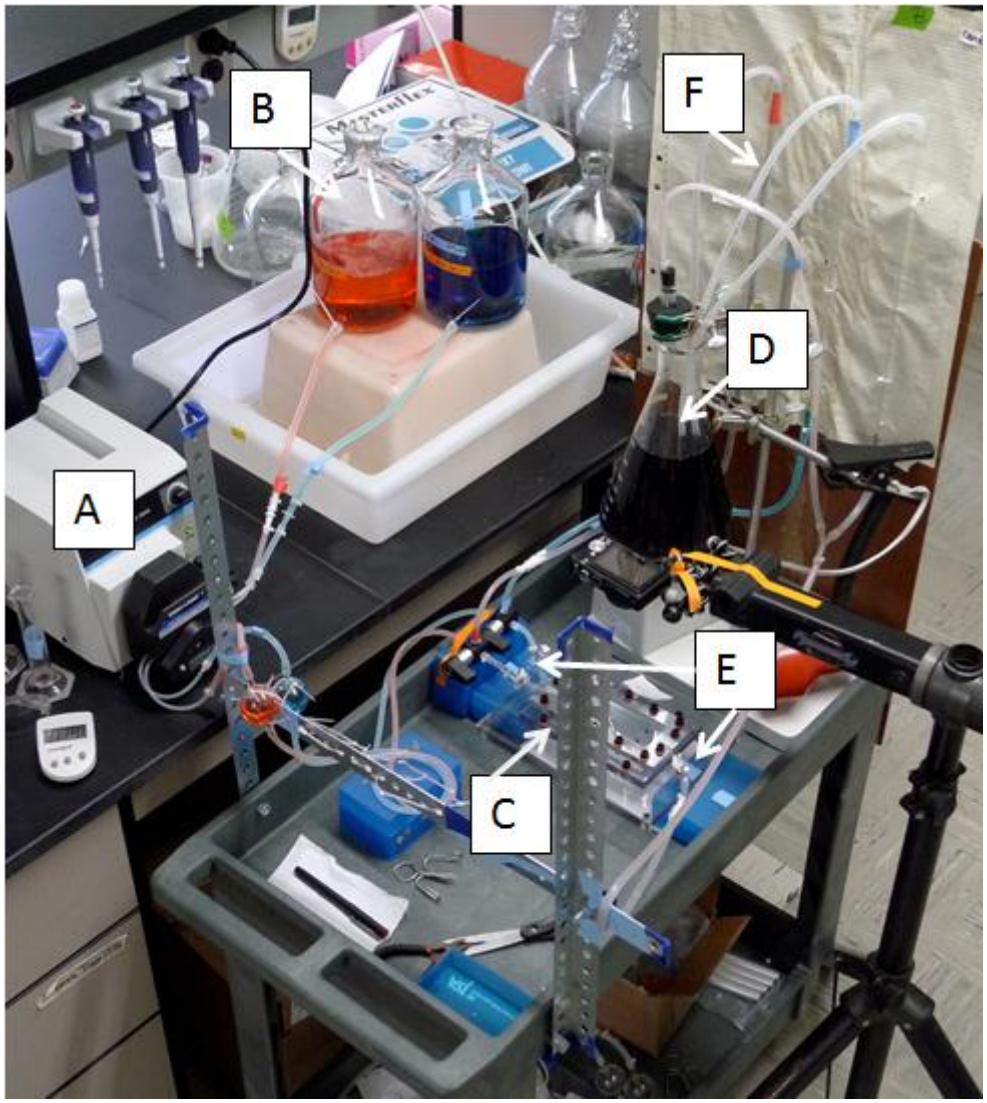

Figure 3.2. Photograph of the flow cell reactor with major components. A peristaltic pump (A) delivered media from reservoirs (B) to porous reactor (C) and then to a waste container (D). Injection ports and sample ports (E) were added just upstream and down-stream of the reactor. Piezometers (F) measured pressure head across the flow cell.

The presence of small air bubbles within the porous media chamber of the reactor were an issue in the early stages of the flow cell set up. The bubbles could cause an artificial disruption in the flow paths. They probably arose from a number of sources.

Actions taken to eliminate the bubbles included removing quick disconnects from the flow cell tubing (to prevent air leaking in at the seals), increasing the height difference between the media reservoirs and the rest of the cart, keeping the flow cell itself at the absolute lowest point in the system (so that the hydrostatic pressure would be highest in the flow cell), switching to aspirator bottles with the media feeds at the bottom to decrease the introduction of a local maximum and then minimum in elevation, and the priming (or filling) of the flow breaks with media prior to running. The vertically oriented apertures leading to the piezometers were larger diameter than the horizontal ones. When the flow of disinfectants was first started, the flow was diverted from entering the flow cell itself until after the bulk of large bubbles was seen to exit the piezometers. This procedure was then repeated between disinfectants and when media was started. The flow was diverted or stopped using 4-way valves rather than with pinch clamps which might have created deformation in the tubing and the creation of bubbles. Bubbles that still entered the flow cell were removed by placing the flow cell vertically and gently tapping it against the counter.

To inoculate the flow cell with the test organism the flow was stopped and clamps were placed upstream of injection ports. *E. coli* MJK2 cells washed into CMM with urea or with calcium (as previously described) were injected into the appropriate injection port (1.5 ml each). Clamps were then also placed downstream of the sample port. The flow remained off overnight (18 h) to allow for biofilm growth and cell attachment (Schultz 2010).

During operation, the flow cell was sampled daily at both the influent and the effluent ports located in the tubing just upstream and downstream of the flow cell, respectively (Figure 3.2 E). Analysis of pH, ammonium, calcium and urea were performed as described for the flask studies. In addition, analyses noted below were conducted during the flow cell experiments. Tracer studies were performed by injecting red food dye (McCormick's, 100 µl) into each of two injection ports upstream of the flow cell and collected downstream at the sample port at 1 minute time intervals. Digital photographs (Panasonic, DMC-LX2) were taken of the flow cell during tracer studies to show the flow paths followed by the dye. Collected samples were diluted and analyzed on a spectrophotometer at 450 nm. Peak breakthrough of the dye was correlated to effective pore volume using a graph of dye intensity versus volume (flow rate multiplied by time).

Piezometers consisted of glass tubing branching out of lines just before and just after the flow cell (Figure 3.2 F). The piezometers were monitored to observe pressure head changes across the flow cell. Tubing extended from the top of the glass piezometers to the waste container so that during initial set up bubbles could be forced out the manometers (rather than entering the flow cell) and also so that during temporary plugging events spilling did not occur out the top of the piezometers. During the study, when a temporary plugging event occurred, the waste lines were lifted so that the extra pressure would force flow back into the flow cell, essentially extending the study.

Drop plates (Herigstad, Hamilton, and Heersink 2001) were performed for enumeration of viable free cells exiting the reactor. Samples collected from the influent and effluent ports were diluted and aliquoted (10 µl) onto LB plates with gentamicin (10 µg/ml). Plates were counted after overnight growth at 37^{o} C.

For photomicroscopy of the flow cell, a DM2500 upright microscope (Leica, Bannockburn, IL) was used. A Fast 1394 camera (Qican, Surrey, BC, Canada) with a Lamda SC-10 smart shutter from Sutter Instruments (Novato, CA) was used to obtain photographic images using a 20x long working distance objective (Leica, 506247) and GFP filter (Leica, GFP size K, 470-440 nm/525-550 nm) for total magnification of 200x. After the experiment, the flow cell was opened and images were again taken of both the inside of the flow cell and the underside of the top glass plate. Images were processed and false color added using ImageJ software (NIH).

Results

Construction of urease positive GFP organisms

Urease-positive GFP-expressing organisms were constructed for use in visualizing cells during calcium carbonate precipitation studies in a flow cell reactor. The initial GFP containing organisms were *E. coli* AF504*gfp* and *P. aeruginosa* AH298. A previously constructed ureolytic strain (*E. coli* DH5α(pURE14.8)) was used as a source for a PCR amplified insert containing the urease operon. This insert was ligated into an L-arabinose-inducible plasmid (pJN105). The entire plasmid plus urease insert was used to transform the GFP strains (Figure 3.1). After construction of the pJN105 plasmid containing the urease operon the insert was sequenced. The sequence of the urease gene operon in the vector pJN105 was identical to the previously sequenced segments of the DH5α(pURE14.8) *ureDABC* (D'Orazio and Collins 1993). However, according to the current version of KB basecaller that was used to determine the sequence- our insert had two additional nucleotides included at the end of the *ureFG* segment resulting in a 99% match (Figure 4.1). When analyzed with e 3730pop7LR (an older basecalling software) the two *ureFG* segments were identical.

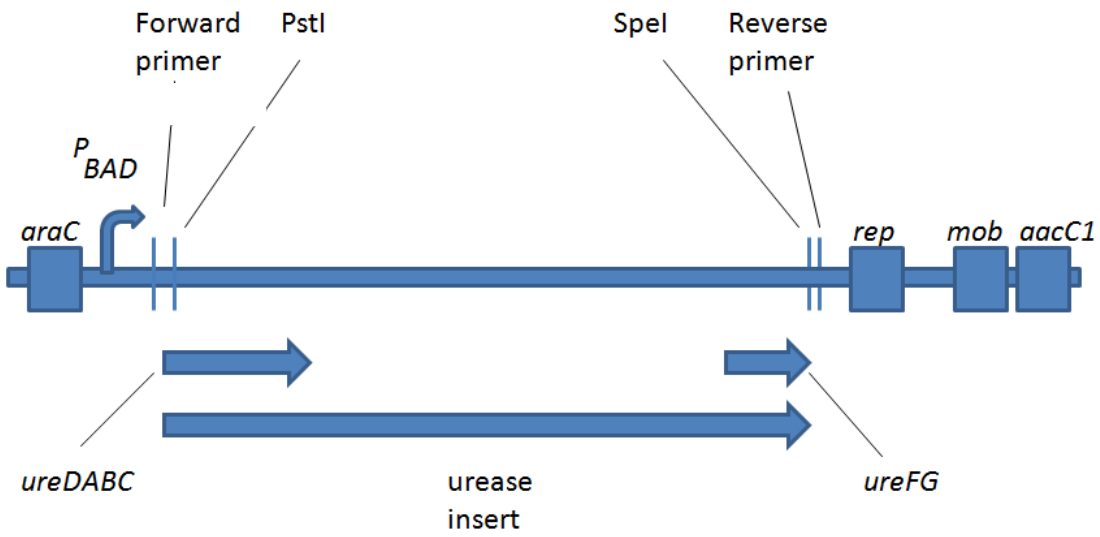

Figure 4.1. Linearized map of vector pJN105 and insert (cloned fragment of DH5α(pURE14.8)). Short arrows *ureDABC* and *ureFG* represent previously sequenced sections of *E.coli* DH5α(pURE14.8). The longer arrow 'urease insert' is the entire section of cloned genes transferred into the pJN105. Restriction sites *PstI* and *SpeI* were added by primers and PCR to the insert to be ligated into the vector pJN105. araC P_{BAD} is the promoter, rep encodes trans-acting replication protein, aacC1 imparts Gm^R, mob encodes the plasmid mobilization functions.

An NCBI BLAST search showed segments with high similarity to *Proteus mirabilis* urease operon (47% E value 0.0), *Vibrio fischeri* ES114 chromosome I (44% E value 0.0) and to other organisms (Zhang et al. 2000) (Table 4.1). Additional similarities in sequence were detected but not included in the table due to low query coverage (small amount of our insert matched an existing sequence) and/or percent identity (percent of

nucleotides that were similar within the matching section). The sequence of the entire cloned fragment can be found in Appendix A.

Table 4.1. BLAST results for sequenced insert (urease operon) in vector pJN105 using KB basecaller. Query coverage refers to the amount of the insert that was similar in sequence to an existing sequence. Percent identity is the percent of nucleotides that were similar within the matching section. Additional sequence similarities with less than 4% coverage were also obtained but not shown here. Cds refers to coding region of a sequence and is usually accompanied by a completeness qualifier.

BLAST hits with significant alignments	**Query coverage (%)**	**Identity (%)**
E.coli urease gene cluster: urease accessory protein D (*ureD*), urease subunits A (*ureA*), and B (*ureB*) genes, complete cds; urease subunit C (*ureC*) gene, 5' end cds	31	100
E.coli urease gene cluster: urease accessory protein F (*ureF*), 3' end cds; urease accessory protein G (*ureG*) gene, complete cds	17	99
Proteus mirabilis strain HI4320, complete genome	47	79
P.mirabilis urease operon: *ureA-ureF* genes, complete cds	47	79
Vibrio fischeri MJ11 chromosome I, complete sequence	29	80
V. fischeri ES114 chromosome I, complete sequence	44	79
Pseudoalteromonas haloplanktis str. TAC125 chromosome I, complete sequence	19	72
Methylotenera sp. 301, complete genome	7	77
E.coli transcriptional activator (*ureR*) gene, complete cds	2	100
Acinetobacter sp. ADP1 complete genome	8	75
Uncultured organism clone 090902CT100S_15 urea amidohydrolase (*ureC*) gene, partial cds	3	83

Transformed strains MJK1 and MJK2 were tested in urea broth with 50 mM L-arabinose (to induce the plasmid) for indication of ureolysis. The urea broth tests showed positive results for ureolysis in both strains (Figure 4.2). Non-transformed strains did not indicate ureolysis (Figure 4.2). The broths also showed evidence that L-arabinose induced the level of urease activity as expected based on plasmid construction (data not shown).

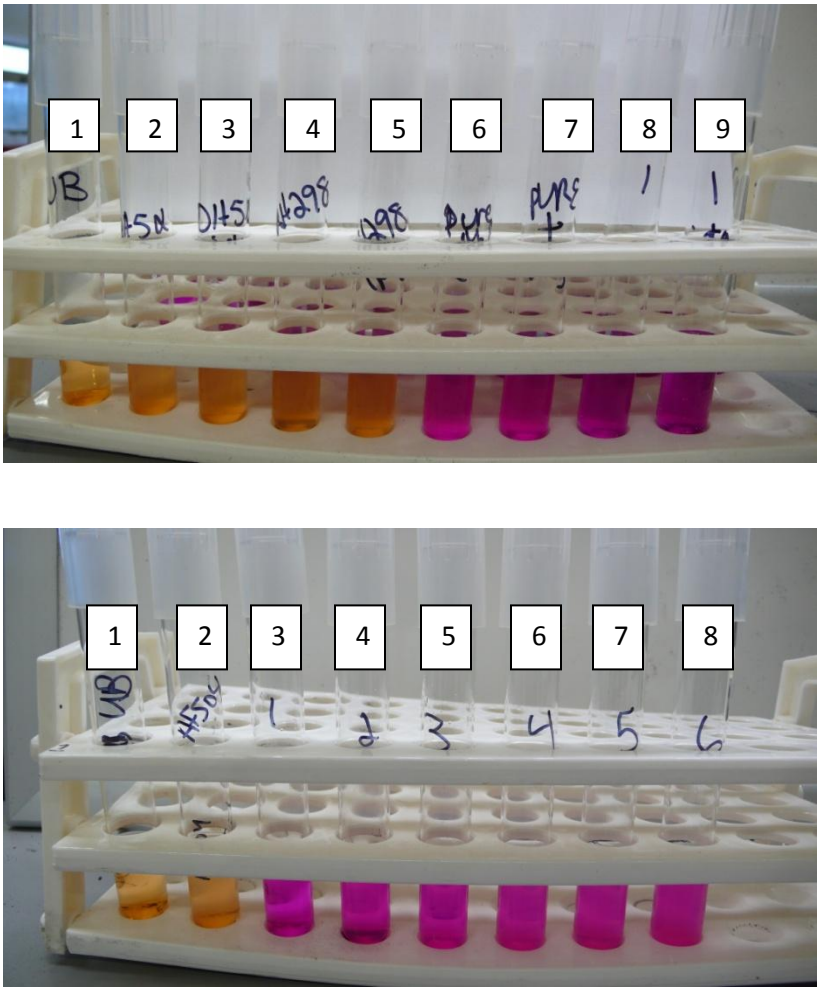

Figure 4.2. Urea broth test results. Pink color indicates urea hydrolysis in a pH sensitive broth test. L- arabinose was added to all tubes at 50 mM. Top image from left: (1) Uninoculated urea broth, (2 and 3) duplicates of negative control DH5α and (4 and 5) AH298, (6 and 7) positive control DH5α(pURE14.8) and (8 and 9) test clone of MJK1. Bottom image from left: (1) uninoculated urea broth, (2) negative control AF504*gfp*, (3-8) clones of transformed MJK2.

Results of ureolysis batch studies

When grown in appropriate media, cells capable of ureolysis and subsequent calcium carbonate precipitation should increase the solution pH, due to the increase in

ammonia that is cleaved from urea, and a decrease in dissolved calcium due to its precipitation in calcium carbonate from solution. Urea levels should also decrease over time due to hydrolysis by the urease enzyme. While the organisms MJK1 and MJK2 showed positive results in urea broth tests, once in the flask environment with CMM base complete without nickel the performance was less obvious (Figure 4.3). The figure below shows a representative example where pH did not increase substantially relative to the negative control (pH of 6.3). The pH would be expected to rise at least as much as the positive control DH5α(pURE14.8) (pH of 9.28) but did not (reaches only 8.17). In addition, not much visible precipitation occurred in the flask. Results for urea, calcium and ammonium similarly showed some but not necessarily strong ureolysis activity (data not shown).

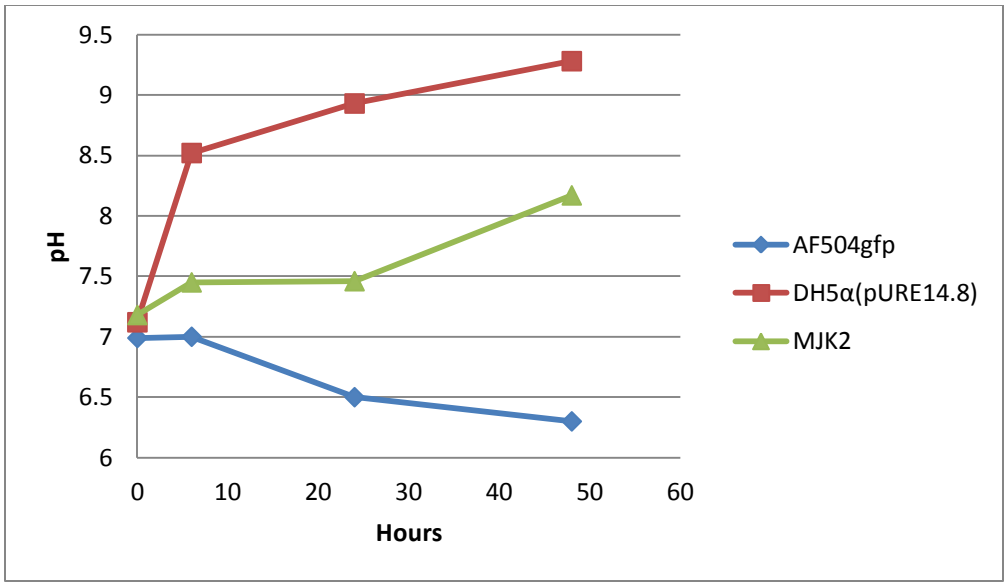

Figure 4.3. pH of flask in an early ureolysis batch study in CMM base complete without nickel. Media contains 50 mM L-arabinose and appropriate antibiotics. No error bars are present, experiment was not performed in triplicate. Organism designations are AF504*gfp* (diamond), DH5α(pURE14.8) (square) and MJK2 (triangle).

In ureolysis batch studies done with CMM base complete (with nickel added, Table 3.1) and 50 mM L-arabinose the new urease transformants performed well. In those cases (performed in triplicate) both MJK1 and MJK2 showed strong ureolytic activity and calcium carbonate precipitation. The non-transformed AH298 or AF504*gfp* still did not perform any measureable ureolysis or calcium carbonate precipitation.

The pH in the flasks remained low in the negative control (non-transformed) organisms. On day 3 they remained on average at 6.48 for MJK1 and 7.43 for MJK2. The pH increased rapidly, however, in the DH5α(pURE14.8) (average of 9.26) and the two

transformants (averages of 9.16 for MJK1 and 9.54 for MJK2) (Figure 4.5). The pH of the MJK2 even exceeded that of the positive control DH5α(pURE14.8).

Ammonium followed the same trend, with even more of a difference between the MJK2 and the DH5α(pURE14.8) (Figure 4.6). By day 3 the average values of the non-transformed organisms were below detection for both MJK1 and MJK2. The actual values were negative when referenced to the standard curve and reflect the error inherent in the Nessler method. In contrast, ammonium values for the DH5α(pURE14.8) reached an average of 2,963 mg/L. The transformed organisms were on average 1,830 mg/L for MJK1 and 7,195 mg/L for MJK2 (Figure 4.6).

Calcium in solution remained highest in the negative control (non-transformed) organism flasks. These averages on day 3 were 991 mg/L for MJK1 and 1,031 mg/L for MJK2. Calcium precipitated out of solution in the transformants falling to averages of 69 mg/L for MJK1 and to 34 mg/L for MJK2. The calcium concentration for positive control DH5α(pURE14.8) averaged 32 mg/L (Figure 4.7). Calcium precipitation can be seen at the bottom of the flasks after the experiment (Figure 4.4).

Trends for urea measurements also suggest that the MJK2 out-performed the positive control in urea hydrolysis. Urea was added to the broth at 20,000 mg/L. On day 3 the non-transformed negative control organisms maintained urea at levels of 20,174 mg/L for AH298 and 16,528 mg/L for AF504*gfp*. The transformants, however, had dropped to 16,411 mg/L urea for MJK1 and to 8,602 mg/L for MJK2. The positive control

DH5α(pURE14.8) had decreased to 13,412 mg/L urea (Figure 4.8). The reason that the MJK2 strain contained more urea than the others on day 1 is not know. Only one replicate was analyzed for urea on the HPLC whereas the other analyses pH, ammonium and calcium used three replicate flasks.

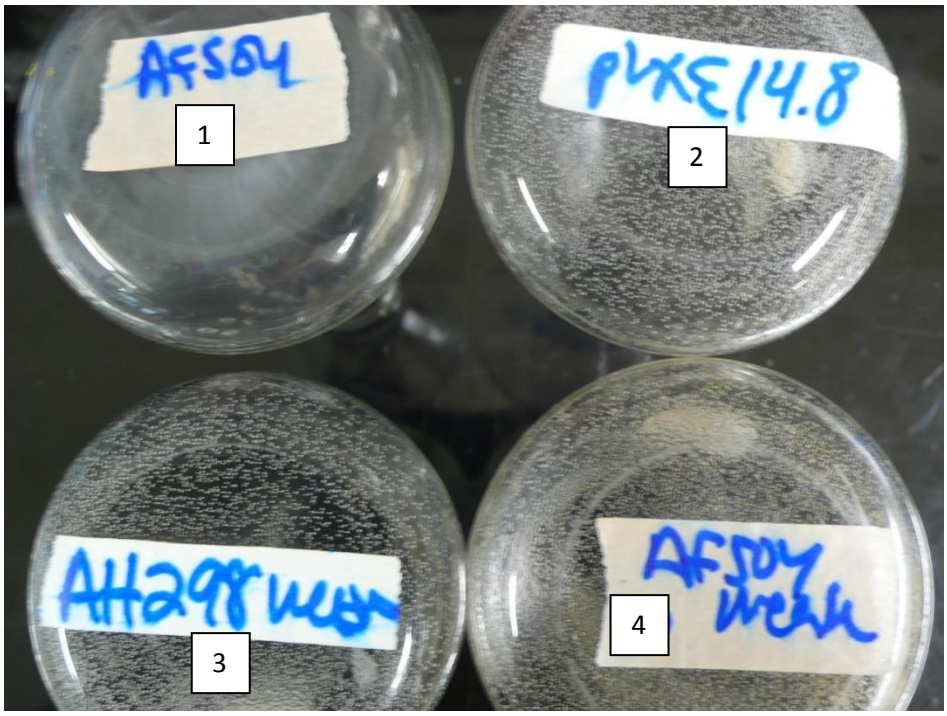

Figure 4.4. Photograph of the bottom of flasks showing relative amounts of calcium carbonate precipitation after 3 days in CMM base complete with 50 mM arabinose. (1) negative control AF504*gfp*, (2) positive control DH5α(pURE14.8), transformants (3) MJK1 and (4) MJK2.

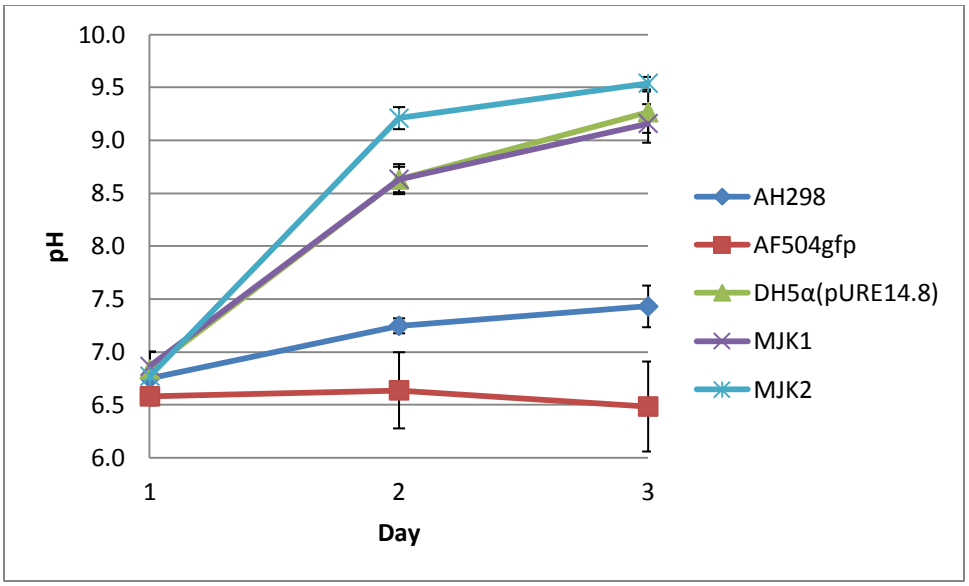

Figure 4.5. pH analyses during ureolysis batch studies. pH levels of medium containing organisms as noted in CMM base complete over 3 days with 50 mM arabinose. Error bars are the standard deviations from triplicate studies. Organism designations are AH298 (diamond) and AF504*gfp* (square) (non-transformed, negative controls), *E.coli* DH5α(pURE14.8) (triangle) (positive control) and MJK1 (cross) and MJK2 (star) (transformed organisms).

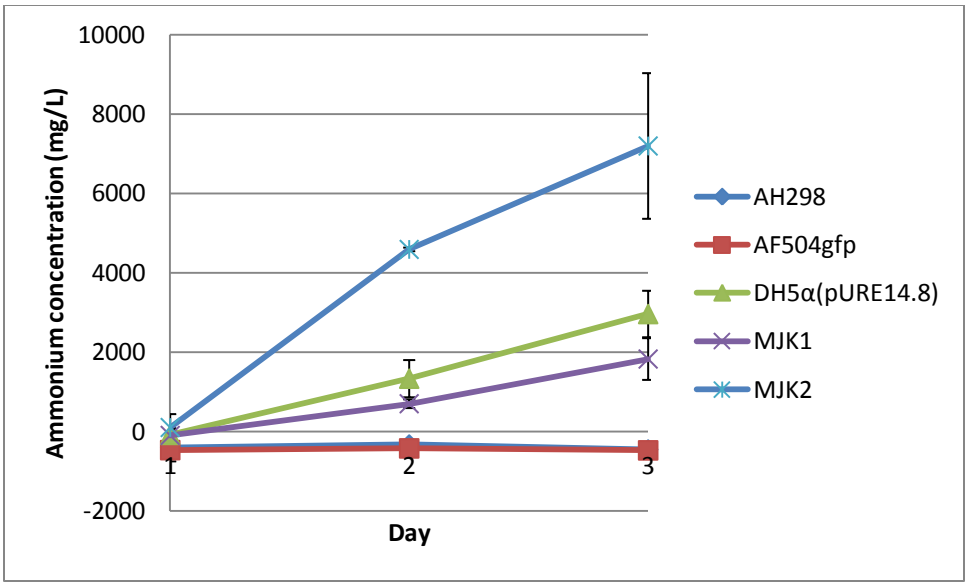

Figure 4.6. Ammonium analyses during ureolysis batch studies. pH levels of medium containing organisms as noted in CMM base complete over 3 days with 50 mM arabinose. Error bars are the standard deviations from triplicate studies. Organism designations are AH298 (diamond) and AF504*gfp* (square) (non-transformed, negative controls), *E.coli* DH5α(pURE14.8) (triangle) (positive control) and MJK1 (cross) and MJK2 (star) (transformed organisms). Negative values portrayed in figure indicate the uncertainty associated with the Nessler assay and these values cannot be distinguished from the zero ammonium standard.

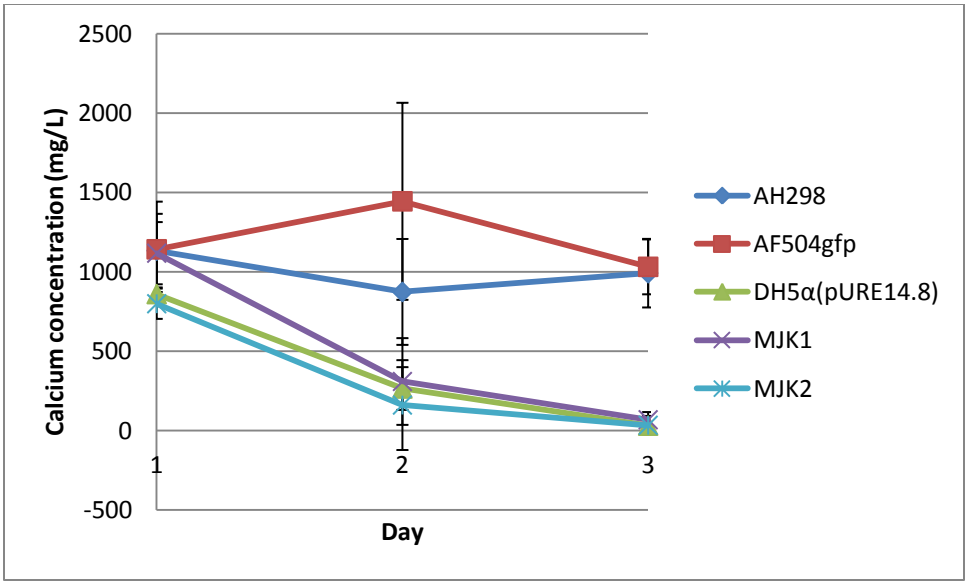

Figure 4.7. Calcium analyses during ureolysis batch studies. pH levels of medium containing organisms as noted in CMM base complete over 3 days with 50 mM arabinose. Error bars are the standard deviations from triplicate studies. Organism designations are AH298 (diamond) and AF504*gfp* (square) (non-transformed, negative controls), *E.coli* DH5α(pURE14.8) (triangle) (positive control) and MJK1 (cross) and MJK2 (star) (transformed organisms).

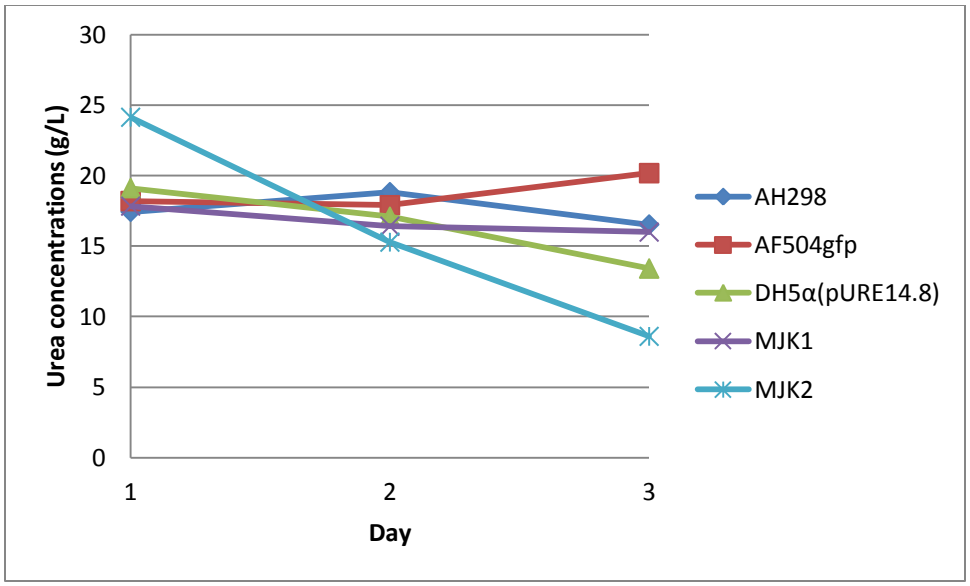

Figure 4.8. Urea analyses during ureolysis batch studies. pH levels of medium containing organisms as noted in CMM base complete over 3 days with 50 mM arabinose. Urea analysis was not measured in triplicate, therefore there are no error bars present in the plot. Organism designations are AH298 (diamond) and AF504*gfp* (square) (non-transformed, negative controls), *E. coli* DH5α(pURE14.8) (triangle) (positive control) and MJK1 (cross) and MJK2 (star) (transformed organisms).

Ureolytically driven calcium carbonate precipitation in the flow cell

The 2D flow cell was inoculated with the newly constructed urease-positive, GFP transformant MJK2 to determine if the organism would drive calcium carbonate precipitation within the flow cells. Images below show daily progression in growth and apparent precipitation within the reactor over the seven-day incubation. Biomass within the flow cells started growing overnight after the inoculation and precipitation can be seen early in the center of the flow cell as the accumulation of particulate matter and later spreading throughout the flow cell (Figure 4.9). The red medium corresponds to

CMM base with calcium and blue is CMM base with urea. Where they come together in the mixing zone (purple in a clean cell) all the components necessary for calcium carbonate precipitation should be present (CMM base complete). Rapid changes occurred in the mixing zone over the first two days especially, followed by a slower progression of change from days 3-7 until the flow eventually became blocked. This mixing region is seen to increase in width with the presence of the ureolytic MJK2 cells even by day 3. This increase in width was approximately from 0.6 cm to 1.3 cm.

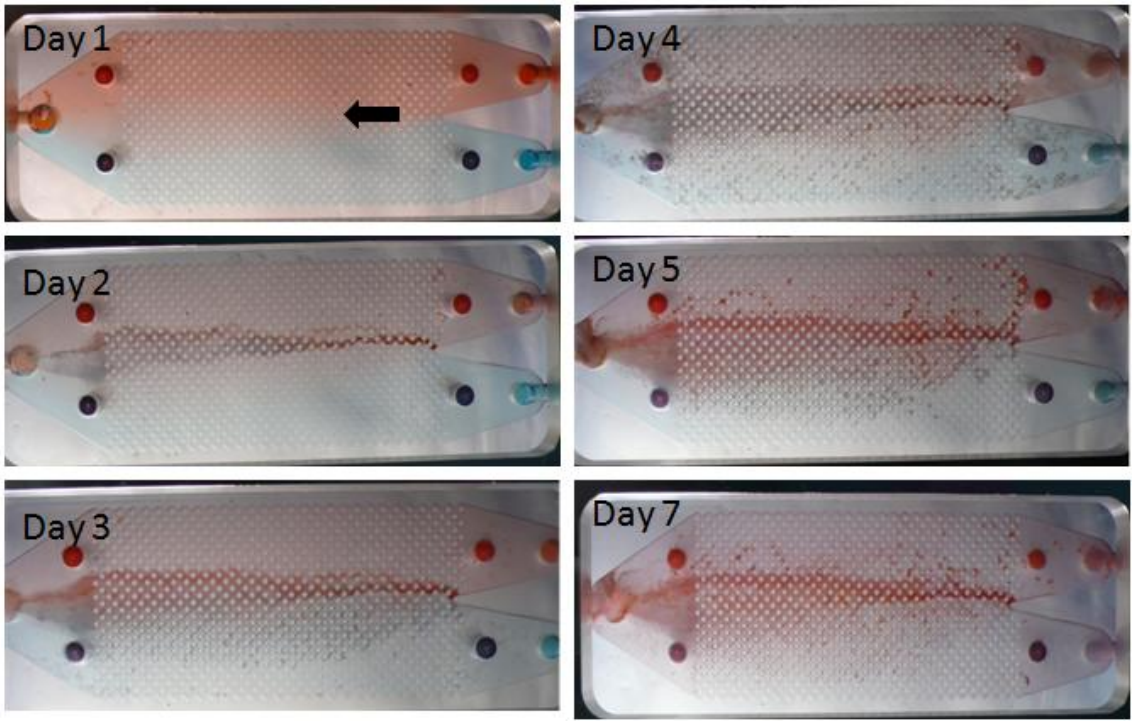

Figure 4.9. Flow cell images (top view) during ureolytically driven calcium carbonate precipitation. Separate panels are labeled with day of the study. Parallel flow is from right to left (as arrow indicates) where blue is CMM base with urea and red is CMM base with calcium. Mixing zone (purple) would make CMM base complete.

Tracer studies allow flow paths to be visualized and for the effective pore volume of the reactor to be quantified. A tracer study was performed on an uninoculated flow cell running the two complementary types of media (blue was CMM base with urea, red was CMM base with calcium) (Figures 4.10 and 4.11). The resulting flow paths and volumes can then be compared to similar data collected during a tracer study on day 3 after inoculation with MJK2, after growth and precipitation had occurred in the flow cell (Figures 4.12 and 4.13).

The series of photographs taken at 2, 4, 5, 10, 20, and 30 minutes of an uninoculated flow cell shows that the dye avoids the very middle line of the reactor and does not appear to mix (Figure 4.10). The blue dye associated with CMM base with urea is just visible exiting the left of the flow cell at 2 minutes. The plot of the intensity of the dye upon exiting the reactor shows that the dye moves through as expected for a classic tracer study. The calculated effective pore volume from the clean reactor was 13 ml (Figure 4.11). This value includes the tubing between the injection ports and sample ports as well as the flow cell itself.

In images of the tracer study with *E. coli* MJK2 taken on day 3 at 3, 5, 8, 10, 20, and 40 minutes the flow paths are seen to avoid the middle of the flow cell to a greater degree than noted for the uninoculated flow cell. Retention of dye in the middle continues for at least 10 minutes longer than in the clean flow cell (e.g. compare Figure 4.10 at 30 minutes to Figure 4.12 at 40 minutes). The dye exiting the flow cell separated into two peaks (Figure 4.13). The effective pore volume on day 3 calculated by these peak breakthroughs corresponds to 12 and 15 ml. However, the real flow rate for this day was not measured, and was presumably lower than the measured initial flow rate set and measured on day 1. Therefore, the calculated measurement (flow rate times time at peak breakthrough) likely overestimates the true effective pore volume. These estimates again include the tubing between ports as well as the flow cell itself. The difference between the clean reactor (13 ml) and the true day 3 reactor (possibly 12 ml or less) may be up to 1 ml or more.

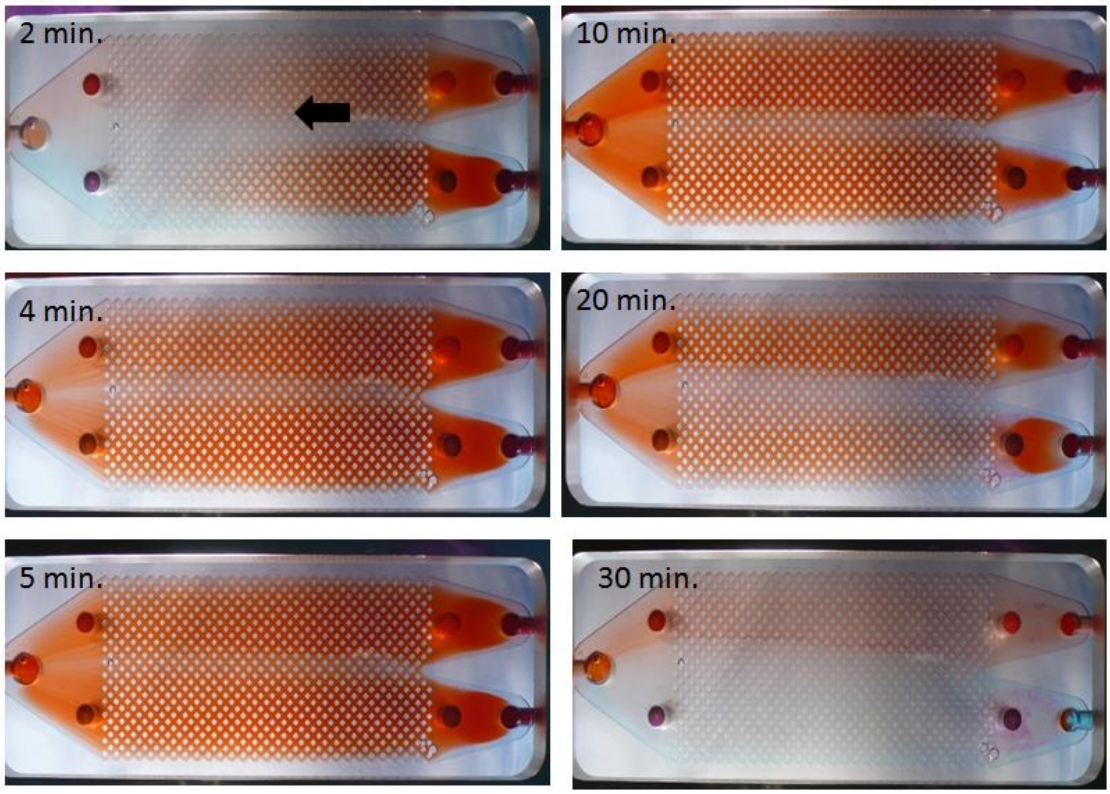

Figure 4.10. Images of flow cell from tracer study on an uninoculated flow cell running parallel flows of complementary media. Images are a top down view. Parallel flows of complementary media for calcium carbonate precipitation (blue is CMM base with urea, red is CMM base with calcium) run from right to left as indicated by arrow. Red dye is injected to both injection ports simultaneously.

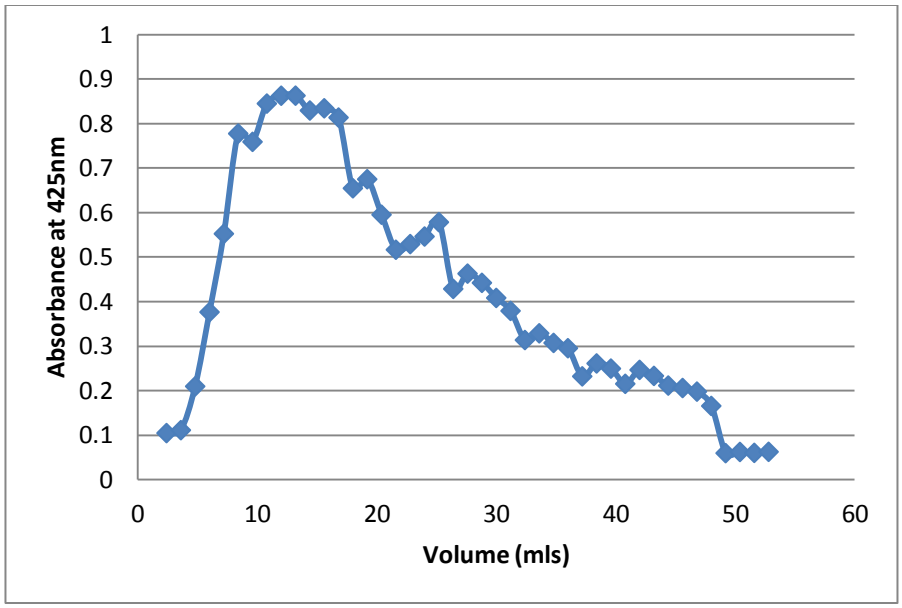

Figure 4.11. Tracer graph shows intensity of red dye upon exiting the flow cell as measured by absorbance at 425nm over the tracer study. The peak of the curve relates to the total volume of porous area remaining in the flow cell including the injection and sample ports.

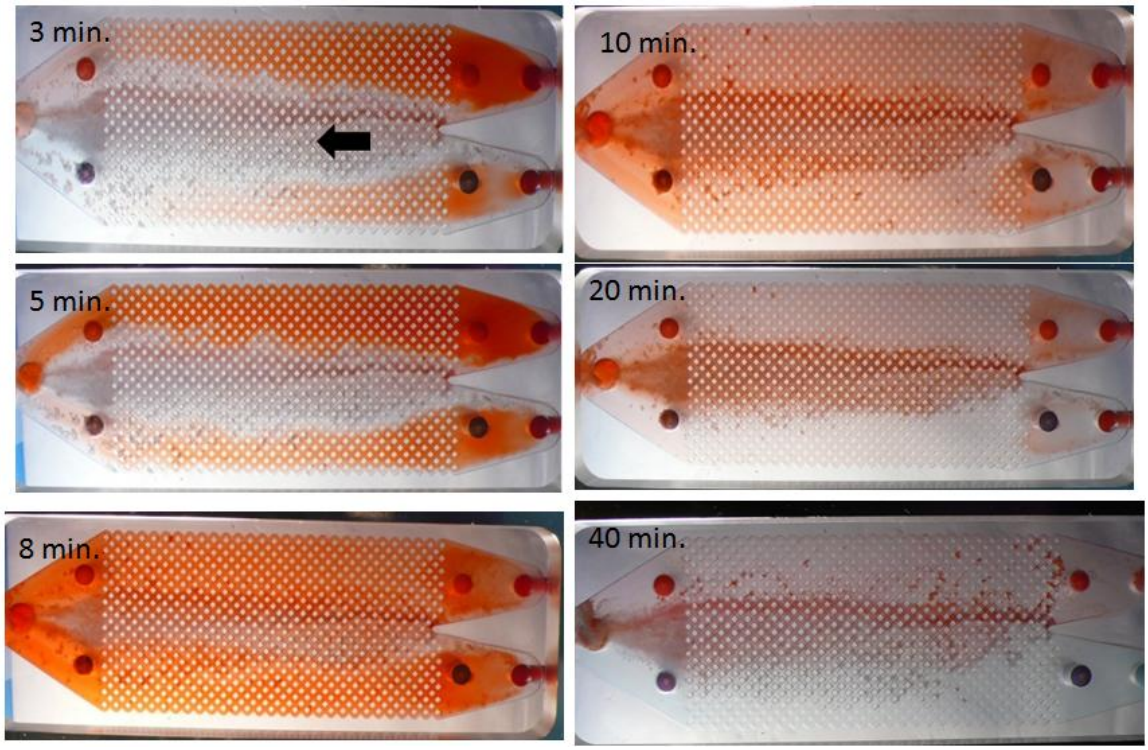

Figure 4.12. Images of flow cell from tracer study on day 3 of ureolytically driven calcium carbonate precipitation. Images are a top down view. Organism is MJK2. Parallel flows of complementary media for calcium carbonate precipitation (blue is CMM base with urea, red is CMM base with calcium) run from right to left. Red dye is injected to both injection ports simultaneously.

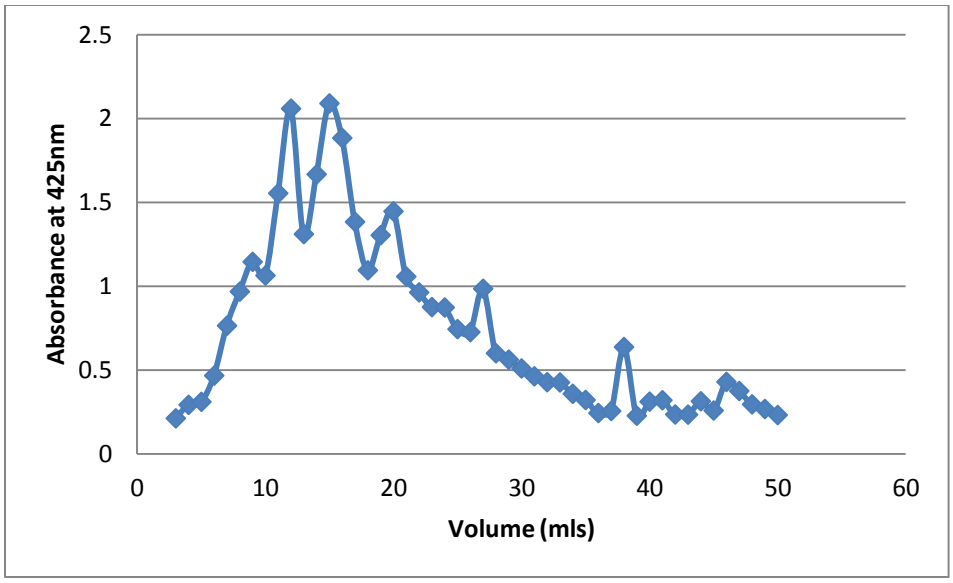

Figure 4.13. Day 3 tracer graph shows intensity of red dye upon exiting the flow cell as measured by absorbance at 425nm over the tracer study. The peak of the curve relates to the total volume of porous area remaining in the flow cell including the injection and sample ports.

The amount of calcium precipitated in four different regions of the flow cell was measured by adding acid to dissolve local precipitates and then recovering the acidic solution and measuring the calcium ion concentration (Table 4.2). If precipitation was occurring preferentially in any of the four quadrants we would expect to see a larger amount of mass collected there. The mass of the two influents combined amounted to more than the mass of the two effluents combined at 4.7 mg versus 1.4 mg calcium dissolved from the region. The total amount dissolved from the reactor was 6.1 mg.

Table 4.2. Mass of dissolved calcium recovered from different regions of the flow cell after demonstration of ureolytically driven calcium carbonate precipitation in parallel flow regime.

Region	Dissolved calcium from region (mg)
Quadrant 1 (influent CMM base with calcium)	1.3
Quadrant 2 (influent CMM base with urea)	3.5
Quadrant 3 (effluent CMM base with calcium)	0.7
Quadrant 4 (effluent CMM base with urea)	0.7
Total in all Quadrants	6.1

Demonstration of ureolytic activity within the flow cell

Samples were collected from the influent and effluent of the flow cell reactors during the study of mixing of two complementary media to determine if the calcium carbonate precipitation observed within the flow cell was driven by ureolytic activity of the MJK2. Results confirmed that ureolysis occurred within the flow cell. pH is expected to be elevated in the effluent compared to influent throughout the time period due to ureolysis occurring within the flow cell and the production of ammonia. This trend was seen, however, the pH was also high in the influent line with CMM base with urea. The peak effluent pH was seen on day 4 (Figure 4.14). In the photographic series of the flow

cell on day 4 precipitation spread throughout the flow cell rather than being concentrated mainly in the middle mixing zone (Figure 4.9).

The ammonium levels also should have remained higher in the effluent with ureolysis occurring in the flow cell. Ammonium levels were higher in the effluent. The effluent concentration of ammonium increased sharply on day 4, and then dropped just as quickly (Figure 4.15) However, ammonium levels were also elevated on days 2, 3, and 4 in the influent containing CMM base with calcium. The reason for this is unknown, but may have been due to the presence of media travelling backwards out of the flow cell as it began to clog.

Calcium concentrations should have decreased from the CMM base with calcium influent as the media exited the flow cell, indicating that calcium had become incorporated to the reactor and precipitated out of solution. Indeed, the effluent levels of calcium remained low throughout the study. The lowest level of calcium in the CMM base with calcium side occurred on day 4. This may have been due to the fact that this influent line was plugged on days 3 and 4 allowing the media to flow from flow cell back into the influent line. The influent with CMM base with urea did not contain calcium so it remained low (Figure 4.16).

Urea should have been highest going into the reactor in the influent containing CMM base with urea but decrease upon exiting the flow cell, again indicating that ureolysis was occurring within the reactor. This is what occurred, with effluent

concentrations of urea reaching low levels on day 4 and the lowest on day 7. Concentrations of the urea in the influent containing CMM base with urea remained high, and the concentrations of urea in the influent containing CMM base with calcium remained low throughout the study.

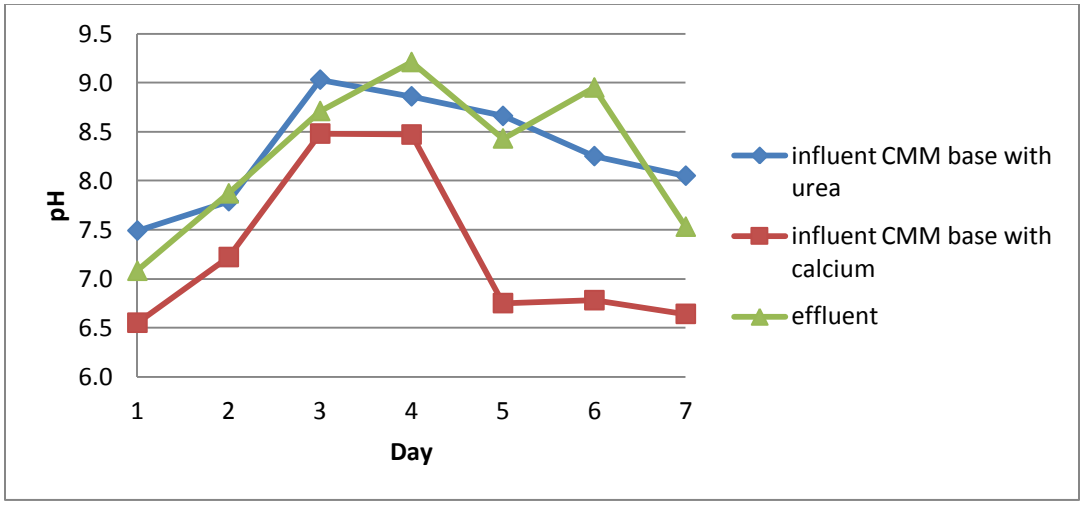

Figure 4.14. pH values recorded during the flow cell study to demonstrate ureolytically driven calcium carbonate precipitation. Samples were taken from both influent ports (CMM base with urea or calcium) and from the effluent port (See Figure 3.2 E). Media designations are influent CMM base with urea (diamond), influent CMM base with calcium (square), and effluent (triangle). Only one replicate was conducted, therefore there are no error bars present on the graph.

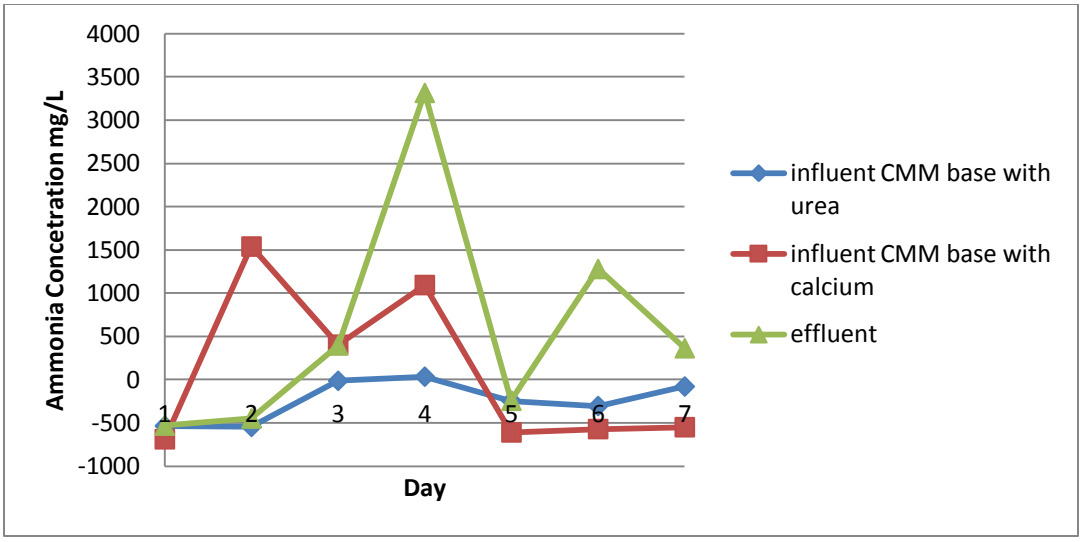

Figure 4.15. Ammonium values recorded during the flow cell study to demonstrate ureolytically driven calcium carbonate precipitation. Samples were taken from both influent ports (CMM base with urea or calcium) and from the effluent port (See Figure 3.2 E). Media designations are influent CMM base with urea (diamond), influent CMM base with calcium (square), and effluent (triangle). Only one replicate was conducted, therefore there are no error bars present on the graph.

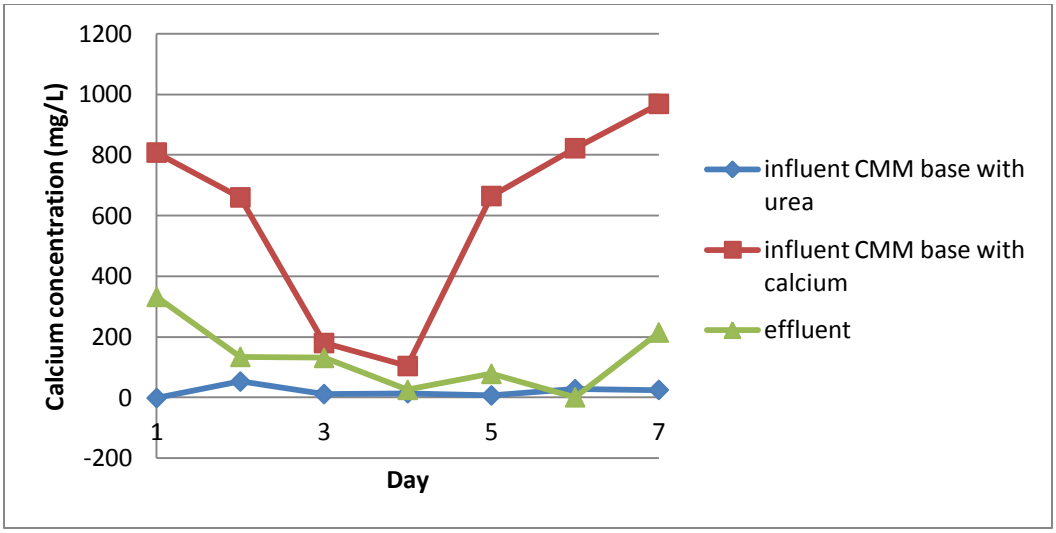

Figure 4.16. Calcium values recorded during the flow cell study to demonstrate ureolytically driven calcium carbonate precipitation. Samples were taken from both influent ports (CMM base with urea or calcium) and from the effluent port (See Figure 3.2 E). Media designations are influent CMM base with urea (diamond), influent CMM base with calcium (square), and effluent (triangle). Only one replicate was conducted, therefore there are no error bars present on the graph.

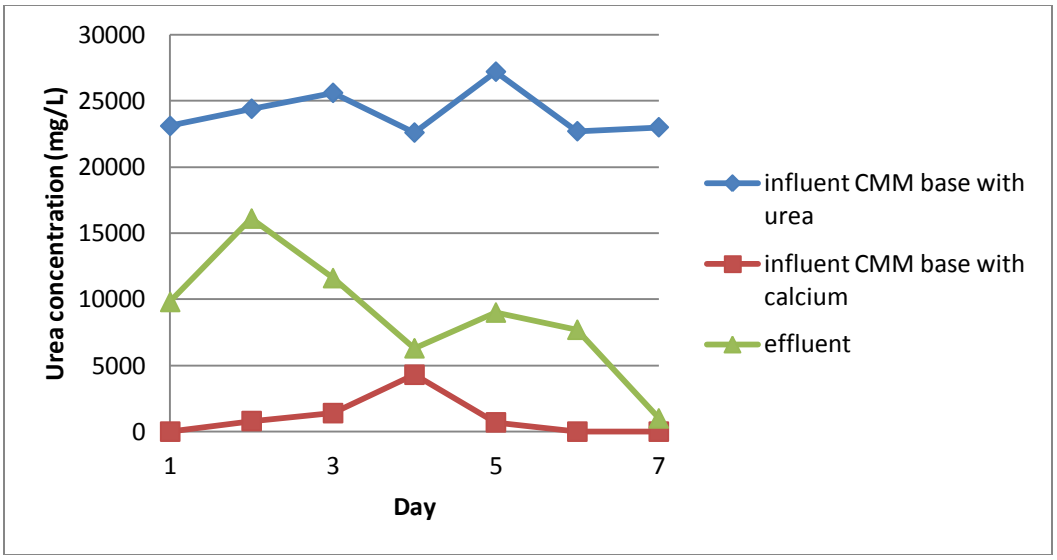

Figure 4.17. Urea values recorded during the flow cell study to demonstrate ureolytically driven calcium carbonate precipitation. Samples were taken from both influent ports (CMM base with urea or calcium) and from the effluent port (See Figure 3.2 E). Media designations are influent CMM base with urea (diamond), influent CMM base with calcium (square), and effluent (triangle). Only one replicate was conducted, therefore there are no error bars present on the graph.

If the flow cell became clogged, then the pressure in the influent ports increased and conversely the pressure dropped or remained stable at the effluent ports. The pressure head increased in the influent line with CMM base with calcium compared to the effluent lines over the entire flow cell study (Figure 4.18). On days 3, 4, 6 and 7 the flow cell became plugged in the influent side containing CMM base with calcium. On days when an influent line was plugged the piezometer overflow lines were lifted to 'reset' the system. This artificially increased the pressure purged the flow cell and restored flow to the flow cell. The influent line containing CMM base with urea remained near the effluent line pressure head until day 5 when it increased. This

increase in pressure head in the line containing CMM base with urea corresponds to the flow continuing through the other line. On days 6 and 7 both lines were plugged and on day 7 the flow could not be reset for either side and so the flow cell was considered permanently plugged and the experiment was terminated.

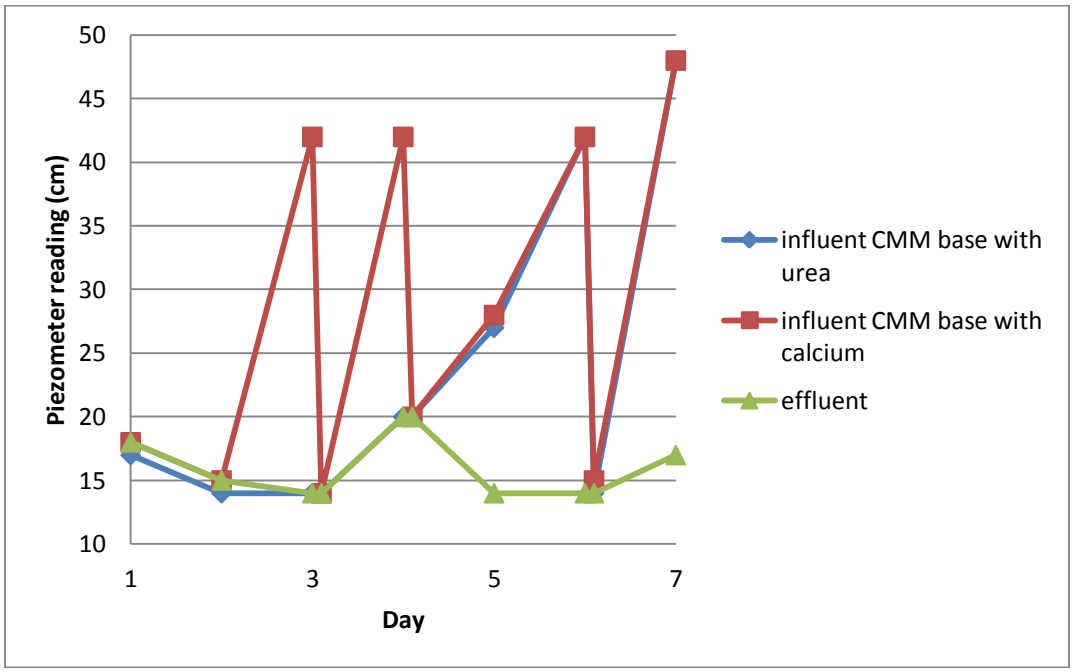

Figure 4.18. Pressure differential across the flow cell during the demonstration of ureolytically driven calcium carbonate precipitation. Points represent measured piezometers readings throughout the experiment. Sharp drops occurring directly after a measured point represent piezometers readings after flow was restored to the flow cell. Resets occurred on days 3, 4, 6 and 7 for CMM base with calcium and on days 6 and 7 for CMM base with urea as needed to continue the experiment. Media designations are influent CMM base with urea (diamond), influent CMM base with calcium (square), and effluent (triangle). Only one replicate was conducted, therefore there are no error bars present on the graph.

To confirm the presence of viable cells, drop plates were performed for the two influent lines (CMM base with calcium or urea) and for the effluent of the flow cell

during the 7 days of the MJK2 flow cell study. The drop plate data showed a viable population exiting the flow cell of 1.8 *10^8 cells/ml at the beginning of the study and 3.8*10^7 cells/ml at the end of the study (Table 4.3). The data also showed evidence that the inoculated cells either remained in or traveled upstream to enter into influent lines as large numbers of viable cells were collected from both influent lines on all occasions sampled.

Table 4.3. Drop plate data for MJK2 in flow cell measured on days 1,2,6 and 7 of the experiment. Colony forming units (CFU) per ml of sampled influent lines (CMM base with calcium or with urea) and the effluent line measured in the flow cell during the demonstration of ureolytically driven calcium carbonate precipitation. (ND is no data).

	CFU/ml (day)			
	1	2	6	7
Influent CMM base with urea	2.4 * 10^7	9.6 * 10^5	ND	8.4 *10^7
Influent CMM base with calcium	1.7 * 10^7	ND	1.6 *10^8	1.2 *10^8
Effluent CMM	1.8 *10^8	ND	ND	3.8 *10^7

No data indicates that growth was observed, however, the number of colonies could not be accurately determined.

Microscopy of the flow cell during demonstration of ureolytically driven calcium carbonate precipitation

Microscopic images were captured of the inside of the flow cell in order to determine the location of MJK2 throughout the demonstration of ureolytically driven calcium carbonate precipitation. Qualitative assessment of the abundance of calcium carbonate in various areas inside the flow cell and over time was also possible. Two-hundred-fold total magnification on a fluorescent microscope with a GFP filter was performed on day 2 and again on day 6.

At the area termed 'first post' (where the two influent media came together) the same exact post was photographed on day 2 and on day 6. On day 2 at the first post there were many microbes visibly present (small bright objects in Figure 4.19 A). Later, on day 6, fewer microbes were visible and the calcium carbonate crystals were larger and more abundant (Figure 4.19 B).

Microbes varied in abundance depending on location in the other regions of the flow cell on day 2. They were quite abundant in the influent mixing region but visibly lower in abundance near the two influent regions. (Compare Figure 4.20 C to Figure 4.20 A or B). Only slight evidence of crystal formation was seen, with the most crystals detected in the two mixing zones. Of these zones the influent mixing zone appeared to have perhaps larger and definitely more abundant crystals. Only a small number of crystals were present in the influent containing calcium (Figure 4.20 A).

As expected, all regions showed more precipitation and larger crystals present on day 6 (Figure 4.21). Again, the influent mixing zone had the most and largest crystals. The effluent mixing zone also contained numerous, large crystals (Figure 4.21 D). The CMM base with calcium had some precipitation present and the CMM base with urea the least (Figure 4.21 A and B). The presence of so much precipitation made it difficult to assess whether the bacteria had decreased in abundance or were just difficult to see due to the co-occurring fluorescence of the calcium carbonate (Figure 4.21).

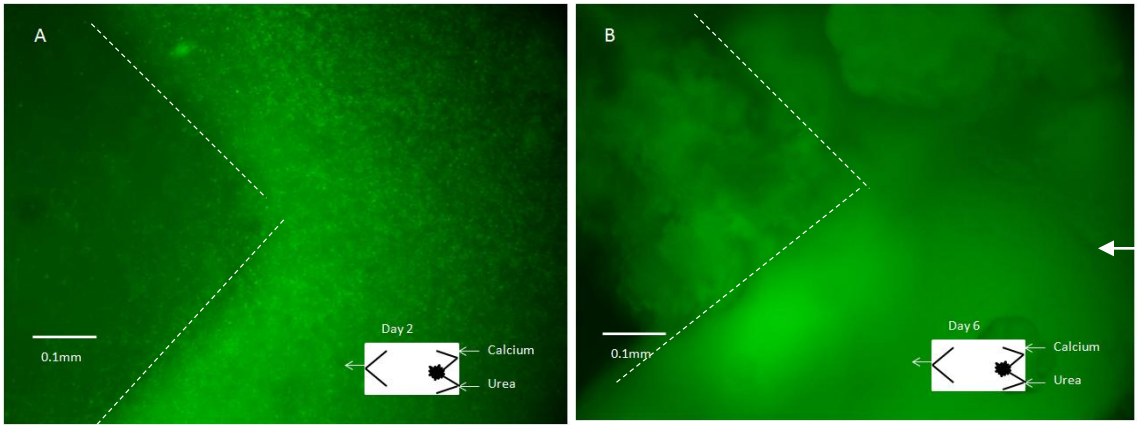

Figure 4.19. Day 2 to day 6 comparison at the first post of flow cell where the two media merge together. MJK2 fluorescing in the flow cell at region specified by inset diagram with 200x magnification and GFP filter on days 2 (A) and 6 (B) of demonstration of ureolytically driven calcium carbonate precipitation. Parallel flows of CMM base with calcium or with urea are from right to left as indicated by the arrows. The brighter green fluorescence relates to a greater cell density or more active cell community (based on GFP production) as well as more or larger calcium carbonate precipitates. Dashed lines roughly outline the sides of the first post on each day.

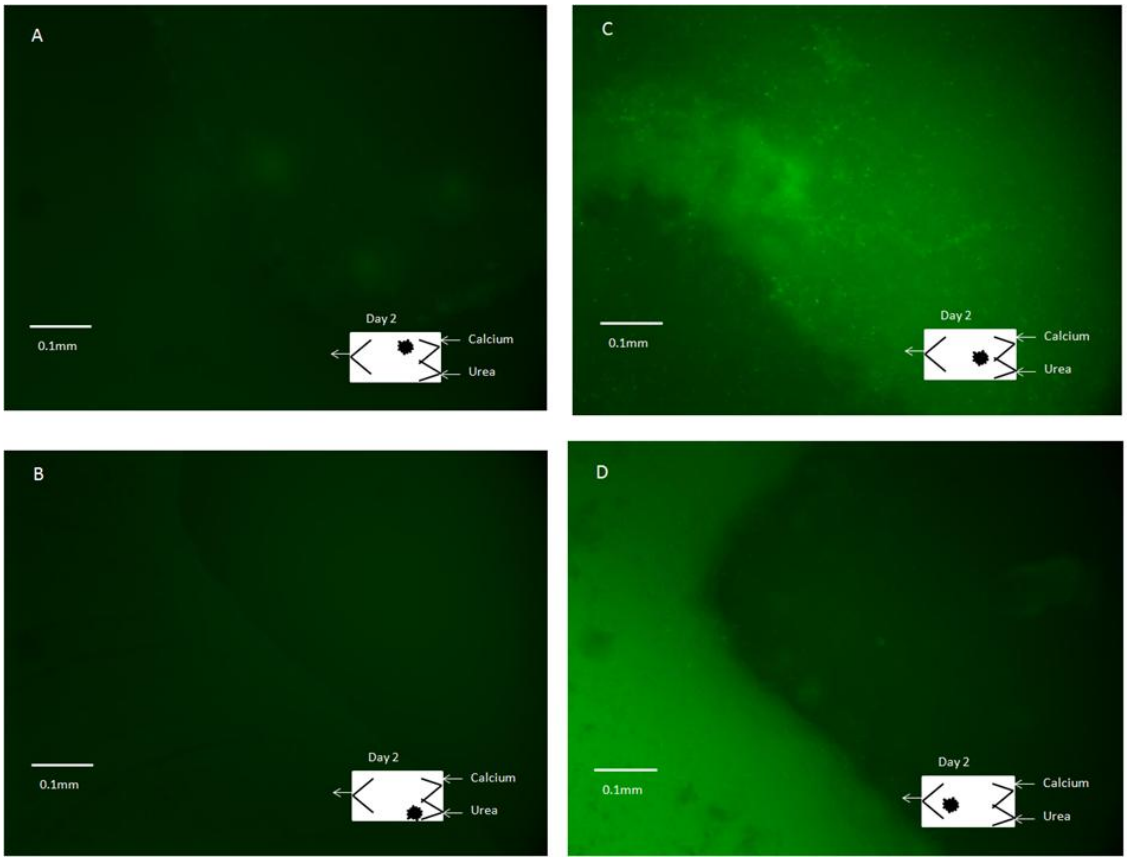

Figure 4.20. Day 2 at various regions throughout the flow cell. MJK2 fluorescing in the flow cell at region specified by inset diagram with 200x magnification and GFP filter on day 2 of demonstration of ureolytically driven calcium carbonate precipitation. Parallel flows of CMM base with calcium or with urea are from right to left as indicated by the arrows. The brighter green fluorescence relates to a greater cell density or more active cell community (based on GFP production) as well as more or larger calcium carbonate precipitates. Locations were near each influent (CMM base with calcium (A) or with urea (B)) and in the mixing zone near the influent (C) or effluent (D) of the reactor.

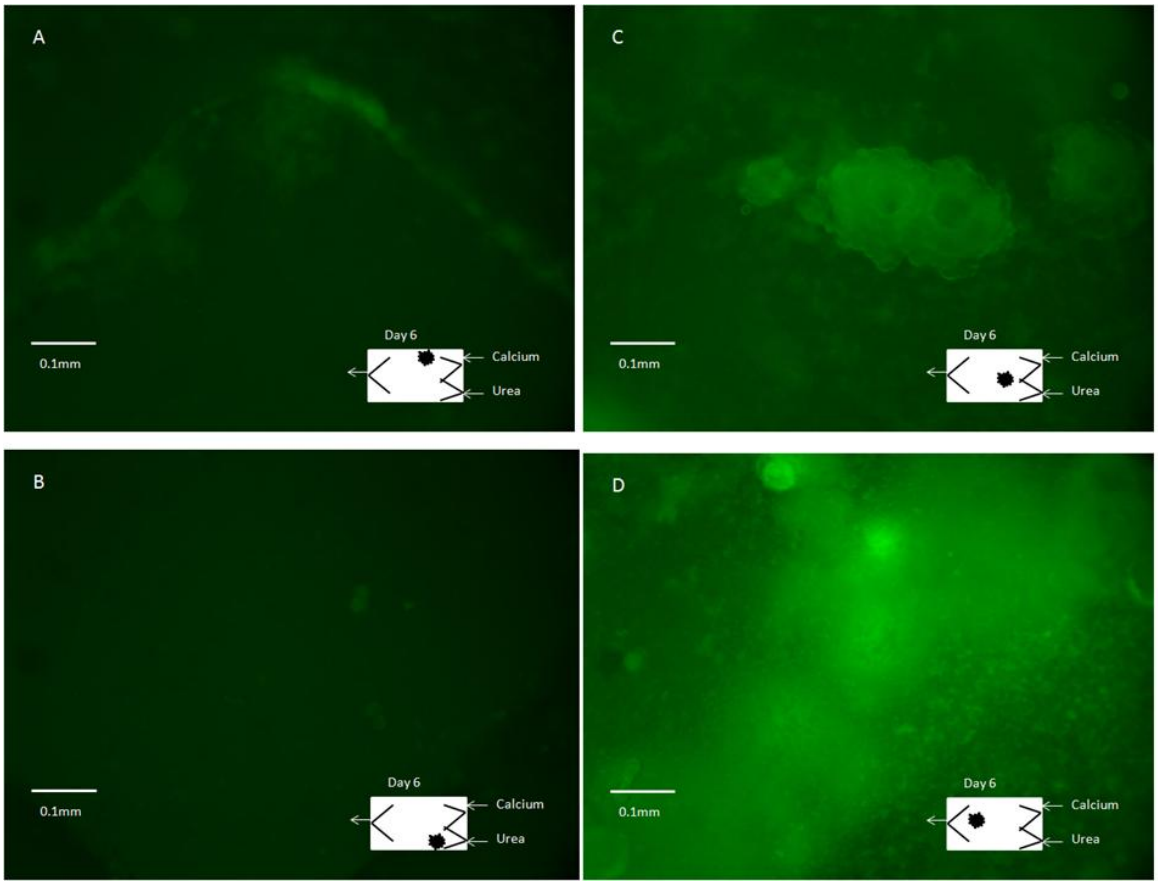

Figure 4.21. Day 6 at various regions throughout the flow cell. MJK2 fluorescing in the flow cell at region specified by inset diagram with 200x magnification and GFP filter on day 6 of demonstration of ureolytically driven calcium carbonate precipitation. Parallel flows of CMM base with calcium or with urea are from right to left as indicated by the arrows. The brighter green fluorescence relates to a greater cell density or more active cell community (based on GFP production) as well as more or larger calcium carbonate precipitates. Locations were near each influent (CMM base with calcium (A) or with urea (B)) and in the mixing zone near the influent (C) or effluent (D) of the reactor.

Discussion

Construction of urease positive GFP organisms

The construction of a model organism that was both ureolytic and contained GFP was desired for use in calcium carbonate precipitation studies within flow cell reactors. This organism could be visualized *in situ* while various studies of flow regimes were being carried out. The resulting information would lead towards optimization of remediation efforts where radionuclides or other metals could be co-precipitated into calcium carbonates.

In early attempts to build this model organism several different organisms and approaches were used. One such scheme included using urease genes from DH5α(pURE14.8) which were PCR amplified (as in the final construction) but with *SpeI* restriction sites on both ends. This allowed for ligation into a pMF54 plasmid at the *XbaI* site (Franklin et al. 1994) along with the red fluorescent protein mCherry. The pMF54 plasmid is repressed by LacI but once derepressed through the addition of IPTG, the promoter should have expressed not only the urease operon but also the mCherry. If transformed into an existing GFP organism, the resulting transformant would theoretically fluoresce green when growing and red when producing urease. However, after construction of the plasmid plus urease insert no ureolytic activity was observed (data not shown). This may have been due to a number of issues that were not investigated further. One possibility is that the insert was cloned in the wrong

orientation. This may have occurred because the same restriction site was on both ends of the insert. However, additional complications with this approach arose when it was discovered that there was an incompatibility in the antibiotics used to maintain the plasmid and the planned GFP organisms to be transformed. The *E. coli*AF504*gfp* strain actually contained an ampicillin resistance gene on its chromosome along with the insertion of the GFP (Folkesson et al. 2008). This problem could be addressed by eliminating the ampicillin resistance gene, or by adding a new antibiotic resistance gene to the plasmid. Instead, a more direct approach was chosen for this thesis work.

In this work both *E. coli* AF504*gfp* and *P. aeruginosa* AH298 (both GFP organisms) were transformed with a pJN105 vector carrying PCR amplified urease genes from *E. coli* DH5α(pURE14.8) ligated at the *PstI* and *SpeI* restriction sites as described earlier (Figures 3.1 and 4.1). Sequencing of the pJN105 vector with the urease insert revealed the apparent insertion of two nucleotides into the cloned segment of the *ureFG* genes during the cloning of our ureolytic organism. This would most likely be a product of a mistake during the PCR amplification process. However, when the sequence was analyzed with an older basecalling software, there was no difference between the DH5α(pURE14.8) and our insert. Regardless, the constructed organisms were ureolytically active in urea broth tests with the addition of L-arabinose.

Ureolysis batch studies

Beyond the confirmation that the new transformants were ureolytic in urea broth tests, their ureolytic activity was also examined in a calcium carbonate precipitating environment. Batch experiments in CMM base complete with L-arabinose were conducted to compare the urea-hydrolyzing capabilities of the non-transformed GFP organisms AF504*gfp* and AH298 with DH5α(pURE14.8) and the transformed urease strains MJK2 and MJK1. Evidence that the transformations were successful was noted by the appropriate changes in pH, ammonia, calcium, urea and by the presence of visible precipitation in the bottom of the flasks containing the transformants relative to those with the non-transformed strains (Figures 4.4-4.8).

While both of the newly constructed organisms MJK1 and MJK2 possessed ureolytic abilities in the urea broth tests and in flask studies, the MJK2 performed especially well. In all cases where nickel was added supplementally, it even out-performed the DH5α(pURE14.8) strain from which the urease genes were transferred. This may have been due to a higher level of enzyme production from the L-arabinose induced pJN105 plasmid than the constitutive levels of the pUC19 plasmid containing the urease genes in DH5α(pURE14.8). However, this possibility was not investigated. It is also not clear as to why the *E. coli* strains (DH5α(pURE14.8) and MJK2) seem to perform better than the transformed *Pseudomonas* strain (MJK1). One possibility is that *Pseudomonas* maintained some mechanism of control over the plasmid-borne urease

gene. Urease in *P. aeruginosa* is in known to be repressed by the presence of ammonium chloride (Janssen et al. 1982). In an effort to overcome this repression the ammonium chloride that is normally in CMM was removed from the medium in order to de-repress gene expression. If the repression had been post-translational (acting on the protein itself after it is existing in the cell), this might have increased the level of ureolysis, however, this increase was not observed.

The addition of 10 μM nickel to the medium was found to greatly enhance the activity of both transformants. As previously discussed, the activity of urease is dependent on nickel concentration (Mobley 1995; Benini et al. 1999). We found that the control organism DH5α(pURE14.8) did not require additional nickel, whereas the new transformants did require additional nickel for urease activity.

Although nickel is required for bacterial growth (normally in nanomolar concentrations) micro- or millimolar levels can be toxic to cells (Sar et al. 1998). Supplemental nickel has been added to media for ureolytically constructed organisms in the past. For instance, Zhang et al. found that their recombinant urease strain of *Lactococcus lactis* showed the maximum level of urease activity at 250 μM $NiSO_4$. They also reported from the literature that a range of supplemental nickel (from 2.5 μM to 200 μM) has been added to media for growing urease constructs (Zhang et al. 2009). The 10 μM nickel tested for the transformants created in this work fits nicely within that

range. 250 µM nickel was also tested but seemed to not produce any activity from the cells at all. Future work may find a more optimal level of nickel for these constructs.

The activity levels of urease can be compared between organisms using kinetic approximations. Several reported rates of ureolysis for different organisms in different conditions are presented below (Table 5.1). However, it is difficult to draw comparisons between studies due to differing conditions and different units of activity that have been reported. For example, Atkinson and Fisher report a rate of 201,000 mU/mg protein for *B. subtilis* which is higher than the rate reported by Morsdorf and Kaltwasser for *S. pasteurii* of 16,900 mU/mg protein (Atkinson and Fisher 1991; Morsdorf and Kaltwasser 1989). This may be due to different media and supplements. Atkinson and Fisher used glucose and glutamate as the nitrogen source in their study and Morsdorf and Kaltwasser supplied only 20 mM urea. Similarly, the difference between rates reported for *S. pasteurii* by Colwell et al. and by Neighbor may be explained by the different experiment set ups, media and lengths of time over which the studies were conducted (Colwell et al. 2005; Neighbor, personal communication). Colwell et al. added 0.001% molasses as a carbon source and 5.9 nM urea whereas Neighbor's were performed in CMM base complete with 300 mM urea. The method of calculating the rates may also be different. Within a study, however, comparisons can be made. For instance, all of the Neighbor rates reported came from experiments conducted under the same conditions for the different organisms. The Neighbor results match those found in this work in indicating that (of the transformed urease organisms) MJK2 has the

highest rates of ureolysis, followed by DH5α(pURE14.8) then MJK1. However, all of these transformants performed much more slowly than *S. pasteurii,* a finding that corresponds to our other data (not shown).

Table 5.1. Ureolytic rates of microorganisms reported for various studies in the literature. ND is no data.

Organism	Rates of Ureolysis		
	mU/mg protein	fmol urea hydrolyzed/cell/hr	mol NH_{4+}/hr
Sporosarcina pasteurii	16,900 (Morsdorf and Kaltwasser 1989)	1.2x10-4 (Colwell et al. 2005) 4,000 (Neighbor, in prep)	0.0054 (Fujita et al. 2000)
Bacillus subtilis	201,000 (Atkinson and Fisher 1991)	ND	ND
Pseudomonas aeruginosa	1,600 (Janssen 1982)	ND	ND
Escherichia coli DH5α(pURE14.8) (Collins and Falkow 1990)	ND	9.89 (Neighbor, in prep)	ND
Pseudomonas aeruginosa MJK1 (Werner et al. 2004 and this work	ND	3.19 (Neighbor, in prep)	ND
Escherichia coli MJK2 (Folkesson et al. 2008 and this work)	ND	26.9 (Neighbor, in prep)	ND
Groundwater samples from Idaho well	ND	8x10^-5 (Colwell et al. 2005)	ND
Ureolytic bacterial isolates from groundwater	ND	ND	3,840 *per mg protein (Collins and Falkow 1990)

The lower ureolytic rates of the transformed organisms may be preferred for long-term experiments where clogging of systems by *S. pasteurii* may be an issue. Also, beyond comparing the ureolytic rates of the different organisms a broader context is also sometimes needed to understand which organism will best serve to address a given research question. Some of the factors that might be of importance are considered for some ureolytic organisms (Table 5.2). The bio-safety level required of the laboratory to use the organism, the original habitat of the organism, and whether it forms biofilms may all be important in determining which organisms to use for a future study. The difficulty of meeting the conditions required for ureolysis to occur at a measurable rate within a certain system may also be of consideration. For instance, *Pseudomonas aeruginosa* and *Bacillus subtilis* have been reported to have ureolytic capability. However, as mentioned earlier great effort was put into determining the conditions under which the urease would be expressed in our calcium carbonate precipitation media but this was unsuccessful. Other organisms also exist which may be used (for example *Helicobacter pylori*) but were not explored due to lacking the GFP biomarker capability, bio-safety issues or due to repression of urease activity by ammonia.

Table 5.2. Comparison of attributes of the ureolytic organisms for use in calcium carbonate precipitation or other studies. Part 1 of 2.

Naturally ureolytic organisms	Growth in biofilms	Ureolytic Activity	Established GFP biomarker	Phylum/Division	Original Environment	Bio-safety level
Sporosarcina pasteurii	Yes (Whiffin 2007)	Very high levels of activity, constitutive regulation (Mobley 1989)	No. Difficult to transform (James Henriksen, personal communication)	Firmicutes (Madigan et al. 2009)	Soil (Madigan et al. 2009)	1
Bacillus subtilis	Yes (Hamon et al. 2004) (Kearns et al. 2005)	In some strains (see table within reference) urease is synthesized at high levels during times of nitrogen limiting growth, specifically when ammonium is limiting (Atkinson and Fisher 1991)	Starvation related stress proteins are activated by sigma B and CIRCE (Bernhardt 1997) Localization tags for fusion of GFP into B. subtilis (Kaltwasser 2002)	Firmicutes (Madigan et al. 2009)	Soil (Madigan et al. 2009)	1
Pseudomonas aeruginosa	Yes (Franklin et al. 2008) (Stapper 2004)	In PA02175 urease is derepressed in times of nitrogen limiting growth. (Janssen 1982 and 1980.) It is under repressible control (Mobley 1989)	rrnBp1 gfp growth rate dependent promoter rpoS GFP construct in biofilm reporting stress (Whiteley 2001)	Gammaproteo-bacteria (Madigan et al. 2009)	Soil, Water (Madigan et al. 2009)	2 or 1 +

Table 5.2. Comparison of attributes of the ureolytic organisms for use in calcium carbonate precipitation or other studies. Part 2 of 2.

Constructed Organisms	Growth in biofilms	Ureolytic Activity/rates	Established Biomarkers/gfp	Taxonomic identity	Original Environment	Bio-safety level
Pseudomonas aeruginosa MJK1 (Werner et al. 2004), (this work)	Yes (Lenz et al. 2008)	Arabinose inducible on plasmid (this work)	Yes rrnBp1 GFP growth rate dependent promoter on chromosome (Werner et al 2004)	Gammaproteo-bacteria (Madigan et al. 2009)	Soil, Water (Madigan et al. 2009)	2 or 1+
Escherichia coli MJK2 (Folkesson et al. 2008),(this work)	Yes (Folkesson et al. 2008) (Wood et al. 2006)	Arabinose inducible on plasmid (this work)	Yes GFP on chromosome (Folkesson et al. 2008)	Gammaproteo-bacteria (Madigan et al. 2009)	Intestine (Madigan et al. 2009)	1
E. coli DH5α(pURE14.8) (Collins and Falkow, 1990)	Yes, flat relatively simple ones (Wood et al. 2006)	Constitutive on plasmid (Collins and Falkow 1990)	No (Collins and Falkow 1990)	Gammaproteo-bacteria (Madigan et al. 2009)	Intestine (Madigan et al. 2009)	1

Ureolytically driven calcium carbonate precipitation in the flow cell

The distribution of ureolytically driven calcium carbonate precipitation is important in determining the effectiveness of various efforts to simulate aquifer remediation pumping regimes. The distribution of calcium carbonate within the flow cell during parallel flow with CMM base with urea or calcium was monitored after inoculation with MJK2. Growth of MJK2 within the flow cell was established and calcium carbonate precipitation resulted. Visual inspection and photographs showed the appearance of precipitation mainly in the mixing zone of the two parallel flows of complementary media. Furthermore, a widening of the mixing zone over time with the presence of the ureolytic organism in the flow cell was apparent by comparing the mixing of media in an uninoculated flow cell (seen as purple dye in photograph Figure 4.9) to the wider distribution of precipitation in the inoculated flow cell as early as day 3 (Figure 4.9). This effect was even more evident on day 4 (Figure 4.9). This increased transverse flow in a porous medium containing heterogeneous regions of low permeability has been modeled using numerical simulations. In one case transverse flow was attributed to flow focusing within the regions of higher permeability (Werth, Cirpka, and Grathwohl 2006). Flow focusing to regions of higher permeability can decrease the distance required for a solute to cross a given number of streamlines increasing mixing rates (Werth, Cirpka, and Grathwohl 2006). This increase in flow to higher permeability areas also causes streamlines to converge and diverge and can lead to plume meandering and transverse flow. The establishment of transverse flow has been

suggested to be integral to the success of *in situ* remediation efforts involving mixing of reactive chemicals or nutrients (Acharya et al. 2007). The introduction of transverse flow in this work leads to enhanced mixing of two complementary media resulting in calcium carbonate precipitation.

This increased area of mixing/reaction was seen in the results of tracer studies as well. The tracer study conducted in the uninoculated flow cell demonstrated low flow in the center region, however, that area is narrower than in the experimental flow cell containing the MJK2 by about 0.7 cm (Compare Figures 4.10 to 4.12). Similar results were found in a simulation study where the mixing of two fluids that cause precipitation altered the dynamics of porosity changes and flow paths (Emmanuel and Berkowitz 2005). In an initially homogeneous environment, they found that if surface area of their model is allowed to increase with decreasing porosity, precipitation is restricted to a fairly narrow band. If instead the surface area of their model is allowed to decrease with decreasing porosity, the region of deposition is wider (Emmanuel and Berkowitz 2005). I did not directly measure surface area changes; however, by analogy with this simulation, the results might imply that in my flow cell, the decrease in porosity by day 3 was accompanied by decreasing surface area. Secondly, when they compared an initially homogeneous domain with an initially heterogeneous one, they found that either way, the formation of impermeable regions in the center of the domain, but that the fluids are able to bypass the region to enable mixing farther downstream (Emmanuel and

Berkowitz 2005). This result was also seen in my flow cell as evidenced by the progressive precipitation downstream over the 8 cm length of the flow cell.

Effective pore volume is a fundamental method of measuring the amount of biofilm growth and calcium carbonate precipitation within a flow cell. The effective pore volume of the flow cell apparently decreased throughout the study, but unfortunately could not be calculated exactly due to an unknown flow rate on day 3 when the tracer study was performed. The decrease in effective pore volume may have been up to 1 ml by comparing the two curves (Figures 4.11 and 4.13). However, if there was any drop in flow rate resulting from the plugging of the reactor, then the calculation of a decrease in effective pore area would be an underestimate and this number could be higher. This decrease in flow rate within the reactor is highly likely since by day 7 flow rate in the reactor was 0 ml/min. Zhang et al. (2010) report on a porous reactor study to drive calcium carbonate precipitation while evaluating permeability reduction. They found, similar to my result that the pore spaces were occluded by calcium carbonate preferentially in the mixing zone of two reactive amendments and that it substantially reduced porosity and permeability (Zhang et al. 2010).

Several factors may have affected the shape of the tracer curve and these factors should be considered in future work. The design of the flow cell injection port (a T entering the flow line) may have been allowed for a longer period of dye bleeding than intended during the study. Also, while not visible to the eye, the density and viscosity of

the dye was probably higher than the media and this may have also created a lag in the time of dye entering the flow cell. Decreasing the dead volume in the injection port and matching the density and viscosity of the dye to that of the media already in the flow cell would respectively address these problems.

The Peclet number is used to describe the quantitative relationship between advection and diffusion plus dispersion (Fetter 1993). The formula for the Peclet number is

$$P_e = (V + L)/D$$

where V is velocity (m/s), L is length (m), and D is the diffusion coefficient (m^2/s). In porous media the diffusion coefficient combines diffusion and dispersion (Fetter 1993). The diffusion coefficient and therefore Peclet number in this work were not determined for this thesis research because the flow rates through the flow cell over time were not measured. Future studies using this flow cell system should include daily measurements of volumetric flow rate so that the Peclet number can be determined.

The attempt to quantify the calcium carbonate precipitated by region within the flow cell was somewhat difficult to interpret. The quadrant approach was not the correct one to take as the middle precipitation zone was divided into all four quadrants and perhaps unevenly. Although we determined that more precipitation occurred near the influent region than downstream near the effluent, a better approach would have been to move along the direction of flow to dissolve regions of calcium carbonate

progressively along the length of the flow cell. In cases of bulk flow (not parallel flow) studies have reported the rapid precipitation and the blocking of the influent preventing downstream precipitation (Lee and Morse 1999; Fujita et al. 2008; Hilgers and Urai 2002). Simulation studies with parallel flow and mixing regimes similar to ours indicate that the inflowing fluids are able to bypass the impermeable regions enabling mixing and precipitation to occur further downstream (Emmanuel and Berkowitz 2005). Future studies where the mass of calcium carbonate precipitated in the flow cell are evaluated from an influent to effluent manner (rather than a quadrant approach) will allow us to compare our studies to one of these two cases.

Demonstration of ureolytic activity within the flow cell

Of primary interest in this demonstration of ureolytically driven calcium carbonate precipitation was the level of ureolytic activity occurring within the flow cell. In analyzing and comparing the pH, ammonium, calcium and urea levels between influent and effluent ports, all of these parameters showed evidence of ureolysis occurring within the flow cell. However, evidence was also found that the ureolysis reactions were occurring in the lines leading to and from the reactor as well. The pH was elevated in the influent line containing CMM base with urea, and ammonium was present in the influent line containing CMM base with calcium. Calcium concentrations decreased in the influent line containing CMM base with calcium especially on days 4

and 5. This evidence of ureolytic activity in the tubing leading into the reactor coincides with the detection of high cell numbers in these influent lines as measured by drop plates. These cells may have been travelling upstream against flow or may have established themselves during the initial shut in period or, being motile, may have travelled upstream during any of the temporary plugging events that occurred on days 3,4, 6 and 7. These pluggings of the flow cell which occurred mainly on the CMM base with calcium influent side were recorded in the piezometers and required a manual 'reset' of flow to the flow cell. Members of R. Gerlach's lab at MSU also have experienced this ureolytic activity in flow cells so much so that at times they had to replace tubing during long-term experiments (E. Lauchnor, personal communication).

Microscopy of the flow cell during demonstration of ureolytically driven calcium carbonate precipitation

The development of the ureolytic GFP organism aided our ability to visualize the interactions between microorganisms, flow paths and precipitation by allowing determination of the location of ureolytic organisms within the flow cell during calcium carbonate precipitation. In the fluorescent microscopy images of the flow cell on day 2 evidence was seen that the constructed *E. coli* MJK2 was present in all areas of the flow cell but especially in the mixing zone and at the first post region (Figures 4.19 and 4.20). By day 6 after more precipitation had occurred within the flow cell the organism could

not be seen microscopically. It is known that calcium carbonate autofluoresces under GFP filters (J. Connolly, personal communication). This autofluorescent interference made it impossible to tell whether the cells were present or to assess their abundance in the various regions.

The microscopy also supported the macro-scale observation that the *E.coli* MJK2 was precipitating calcium carbonate preferentially in the mixing zone (Figure 4.9). The two influent regions and the influent mixing zone of the flow cell examined on day 2 and day 6 showed the most calcium carbonate crystals in the mixing zone each day. Fewer crystals were evident in the flow cell section that received CMM base with calcium and even fewer crystals were seen in the flow cell section receiving CMM base with urea. In a study using similar style flow cell reactors and *S. pasteurii* with bulk flow (not parallel flow) the influent region was similarly found to contain more and larger crystals regardless of location (Schultz 2010). Their crystals showed a gradient of decreasing size towards the effluent (Schultz 2010).

It could be that the GFP cells were not fluorescing as brightly in different regions on day 2 or by day 6 due to biological reasons but this is difficult to assess due to several factors. Even if the GFP organisms can be easily located, care must be taken in assigning too much meaning to the activity levels of fluorescent cells within various regions of the flow cell or throughout the study by comparing apparent differences in GFP intensity. While the ribosome promoter *rrn*Bp_1 is fused with an unstable variant of GFP in the

transformed MJK2 (the unstable GFP (AAV gene) results in a decrease in fluorescence signal intensity when the cells enter stationary phase (Sternberg et al. 1999), the fluorescence may also be dampened by other factors. For instance, lower levels of oxygen. Oxygen gradients have been found to vary dramatically even across small spatial scales in flow cell studies (Stewart and Franklin 2008). Surrounding microcolonies or changes in flow paths may also result in a depletion of nutrients or build up of wastes that could also affect the fluorescence. In addition, differences in metabolic activity within a biofilm have been observed (Werner et al. 2004).

While the GFP may not be able to tell us much about the overall activity of cells within a heterogeneous environment like the flow cell, future studies are likely to find the constructed ureolytic GFP organism helpful. For example, if one is interested mainly in the activity of the cells, they may be able to use the constructed ureolytic GFP organisms within a more controlled, uniform environment such as a 96 well assay plate. In this environment one would be able to measure cellular activity in CMM base with urea, perhaps even varying conditions to optimize activity. Alternatively, future studies interested in cell location and changes to their distributions over time may use my constructed ureolytic GFP strains in a smaller flow model such as a micro flow cell models or capillary tubes as these can be used with a confocal microscope. In these smaller flow cell models more detailed imaging including 3D information may prove ideal for linking the cells' activities and locations in the context of overall distributions of calcium carbonate precipitation.

Future work

My constructed model organisms are unique options within the field of calcium carbonate precipitation. In being both ureolytic and containing a GFP they have considerable potential for laboratory investigations into the relationship between microbial location and activity, resulting calcium carbonate precipitation and subsequent changes in flow paths. The activity level of the urease is lower than for the often used *S. pasteurii* but measurable in a number of situations including urea broths, flasks with CMM, and the flow cell environment. They can form biofilms, even complex ones in the case of the MJK1 strain. They are considered biosafety level 1 or 1+ for laboratory work. They can be visualized during a flow cell experiment. For example, if used as previously mentioned in a smaller flow cell model or in a capillary with a confocal microscope the ability to quantify 3D biofilm growth would answer questions about cellular growth that may be used for computer models that predict behavior of such systems. Alternatively, the GFP may be used as a biomarker for cellular activity if the experiment is conducted in a more uniform environment for GFP such as within a 96 well plate and if great care is given to control for confounding variables that affect GFP fluorescence.

The 2D flow cell models used in this study have potential for interesting future work as well. While I demonstrated the ability of the constructed organism to ureolytically drive calcium carbonate precipitation within the flow cell operated using a

parallel flow regime an important next step would be to examine parallel flow with a non-ureolytic organism. This would separate the growth of the organism versus growth with calcium carbonate precipitation. Going further, I would compare the ureolytic and non-ureolytic organism results with a non-microbially mediated calcium carbonate precipitation situation. For this, one could use a fixed urease enzyme or inject parallel flows of calcium chloride and sodium bicarbonate.

The addition of a second pump to the system, and therefore the ability to independently control parallel flows with differing flow rates would also represent a possible method for increasing the overall mixing area and potential for calcium carbonate precipitation. In this type of a research situation, one could explore the options of pushing one faster flow across the region of slower flow to stimulate mixing.

With the urease GFP organism and with the calcium carbonate precipitation patterns observed from a parallel flow regime data produced are likely to be helpful to modelers when simulating the process to aid in remediation. The results of the model simulations could prompt the next round of experiments, the data from which could be used to make the models even better.

Conclusion

The need to understand more about the pore-scale processes associated with microbially driven calcium carbonate precipitation in porous media led us to construct two ureolytic GFP organisms. Our choice was to add urease genes to the strains *P. aeruginosa* AH298 and *E. coli* AF504*gfp* which already contained an altered, unstable GFP derivative (Folkesson et al. 2008; Werner et al. 2004). Both organisms produced significant levels of urease activity in urea broth tests and in flasks with CMM base complete media for the promotion of calcium carbonate precipitation. We found that urease activity level for the two constructs was dependent upon the addition of supplemental nickel to the medium. Although the reason for this nickel dependency is not entirely clear, this may have been due to two nucleotide insertions that were determined to be present in the sequence of a putative nickel acquiring gene at the end of the PCR amplified gene inserted into the plasmid.

These newly constructed ureolytic GFP organisms join a number of other organisms that may be used to promote calcium carbonate precipitation. The addition of GFP reporting cells and the ability to monitor the location of cells throughout ongoing experiments should prove useful in a wide range of applications including future remediation studies and possibly even the development of models in medical, agricultural or soil-strengthening research.

In this work, the model constructed ureolytic organism MJK2 that contained green fluorescent protein (GFP) was used in a 2D flow cell as a tool to investigate the pore-scale relationship between organisms performing ureolysis and flow paths resulting from subsequent calcium carbonate precipitation. We used a laboratory-scale continuous flow reactor to simulate the porous environment of an aquifer. The GFP allowed the location of active bacteria (those producing ribosomes) to be visualized while carrying out calcium carbonate precipitation through ureolysis in the flow cell chamber without the use of a destructive staining procedure. The flow cell was operated in a parallel flow regime with CMM base with calcium on one side and CMM base with urea on the other. In the mixing zone of the two media calcium carbonate precipitation occurred. Our objective was then to show that the newly constructed organism carried out ureolysis and calcium carbonate precipitation while in the model reactor. We further demonstrated that its presence enhanced the amount of mixing of the two media and promoted a more widespread pattern of calcium carbonate distribution.

The reactor operated with the *E. coli* AF504*gfp*:urease showed evidence of calcium carbonate precipitation and became plugged within 7 days. As hypothesized, a widening of the mixing zone occurred. This was evident when compared to the width of the purple color of mixing in clean cell. We observed a higher number of cells and greater degree of precipitation in the mixing zone as compared to the other regions in photographs as well as microscopically.

The main difficulty in the system as set up was that it was hard to distinguish the fluorescing cells from calcium carbonates that autofluoresced at the same wavelengths. We can foresee either of the constructed organisms being used in future calcium carbonate or ureolytic studies. For instance, in a more uniform environment the GFP may be quantified under different ureolytic conditions to further optimize calcium carbonate precipitation conditions. Alternatively, in a micro flow cell model or capillary the GFP would be visible through a confocal microscope and space filling 3D models of the amount of biofilm present under various conditions may be quantified.

Additional studies will help further the overall goals of optimizing calcium carbonate precipitation distribution within porous media. The 2D flow cells could be operated using a non-ureolytic bacterium to distinguish between changes in flow paths due to growth versus precipitation of calcium carbonate, or with a fixed enzyme urease to compare biologically induced patterns of precipitation to non-microbially mediated ones.

Aquifer remediation after contamination with divalent radionuclides or metals is a problem that requires solutions to improve the health of the environment and for maintaining safe groundwater for people. Microbially enhanced co-precipitation into calcium carbonate is a strategy well suited to many cases and is attractive as a remediation option; however, the optimum way to employ such a method in the field is still unknown. To remove the most contaminant from the water of the aquifer, it is

necessary to avoid plugging the inlet wells where the amendments intended to stimulate microbial calcite precipitation are being added. By understanding more about the interaction of microorganisms that carry out subsurface remediation by altering flow paths and precipitation patterns, we can promote the conditions that cause these remediation strategies to occur gradually and more effectively.

References

Acharya, R. C., A. J. Valocchi, C. J. Werth, and T. W. Willingham. 2007. “Pore-scale simulation of dispersion and reaction along a transverse mixing zone in two-dimensional porous media.” *Water Resources Research* 43 (10) DOI: 10.1029/2007WR 05969

Alabama Department of Environmental Management. "Groundwater Contamination." Accessed November 21, 2011. www.adem.state.al.US/programs/water/groundwater.cnt

Andersen, J. B., C. Sternberg, L. K. Poulsen, S. P. Bjorn, M. Givskov, and S. Molin. 1998. “New unstable variants of green fluorescent protein for studies of transient gene expression in bacteria.” *Applied and Environmental Microbiology* 64 (6): 2240-2246.

Atkinson, M. R., and S.H. Fisher. 1991. “Identification of genes and gene products whose expression is activated during nitrogen-limited growth in *Bacillus subtilis*.” *Journal of Bacteriology* 173 (1): 23-27.

Banfield, J.F., and K.H. Nealson. 1997. *Geomicrobiology: Interactions between Microbes and Minerals*. Vol. 35. Reviews in Minerology. Minerological Society of America.

Bang, S. S., J. K. Galinat, and V. Ramakrishnan. 2001. “Calcite precipitation induced by polyurethane-immobilized *Bacillus pasteurii*.” *Enzyme and Microbial Technology* 28 (4-5): 404-409. DOI: 10.1016/S0141-0229(00)00348-3.

Bengtsson, G. 1989. “Growth and metabolic flexibility in groundwater bacteria.” *Microbial Ecology* 18 (3): 235-248.

Benini, S., W. Rypniewski, K. Wilson, S. Miletti, S. Ciurli, and S. Mangani. 1999. “A new proposal for urease mechanism based on the crystal structures of the native and inhibited enzyme from *Bacillus pasterurii*: why urea hydrolysis costs two nickels.” *Structure* 7 (2): 205-216.

Boquet, E., A. Boronat, and A Ramos-Cormenzana. 1973. “Production of calcite (calcium carbonate) crystals by soil bacteria is a general phenomenon.” *Nature* 246 (5453): 527-528.

Ciferri, O. 1999. *Of microbes and art: the role of microbial communitites in the degradation and protection of cultural heritage*. Vol. Proceedings of an International Conference on Microbiology and Conservation (ICMC). Florence, Italy: Spinger 2000, June 17. http://books.google.com/books?id=IOW9Z5YVFJIC&pg=PA86&lpg=PA86&dq=pseudomonas+aeruginosa+media+calcite+precipitation&source=bl&ots=gm_BjPC5lJ&sig=7pCIJohMtzMvOh7rnJNi_VJZdew&hl=en&ei=ljdjSoTRCJHSsQOT8ZRn&sa=X&oi=book_result&ct=result&resnum=4.

Clark, S., P. S. Francis, X. A. Conlan, and N. W. Barnett. 2007. “Determination of urea using high-performance liquid chromatography with fluorescence detection after automated derivatisation with xanthydrol.” *Journal of Chromatography A* 1161 (1-2): 207-213. DOI: 10.1016/j.chroma.2007.05.085.

Collins, C. M., and S. Falkow. 1990. “Genetic analysis of *Escherichia coli* urease genes: evidence for two distinct loci.” *Journal of Bacteriology* 172 (12): 7138-7144.

Colwell F. S., R. W Smith., F. G. Ferris, A. Reysenbach, Y. Fujita, T. L. Tyler, J.L Taylor., A. Banta, M.E. Delwiche, T.L. McLing and M.E. Watwood. 2005. Microbially mediated subsurface calcite precipitation for removal of hazardous divalent cations: Microbial activity, molecular biology, and modeling. In (E. Berkey and T. Zachary, eds.) *Subsurface*

Contamination Remediation, 904:117-137. ACS Symposium Series. American Chemical Society. http://dx.doi.org/10.1021/bk-2005-0904.ch006.

Cruz-Ramos, H. 1997. "The *Bacillus subtilis* ureABC operon." *Journal of Bacteriology* 179 (10): 3371-3373.

Cunningham, A.B., R.R. Sharp, R. Hiebert, and J. Garth. 2003. "Subsurface biofilm barriers for the containment and remediation of contaminated groundwater." *Bioremediation Journal* 7 (3): 151-164.

Davey, M. E., and G. A. O'Toole. 2000. "Microbial biofilms: from ecology to molecular genetics." *Microbiology and Molecular Biology Reviews* 64: 847-867. DOI: 10.1128/MMBR.64.4.847-867.2000.

de Lipthay, J. R, N. Tuxen, K. Johnsen, L. H. Hansen, H. Albrechtsen, P. L. Bjerg, and J. Aamand. 2002. "*In situ* exposure to low herbicide concentrations affects microbial population composition and catabolic gene frequency in an aerobic shallow aquifer." *Applied and Environmental Microbiology* 69 (1): 461-467.

de Simoni, M., X. Sanchez-Vila, J. Carrera, and M. W. Saaltink. 2007. "A mixing ratios-based formulation for multicomponent reactive transport." *Water Resources Research* 43 (7): W07419.

Dutta, L., H. E. Nuttall, A. Cunningham, G. James, and R. Hiebert. 2005. "*In situ* biofilm barriers: Case study of a nitrate groundwater plume, Albuquerque, New Mexico." *Remediation Journal* 15 (4): 101-111. DOI:10.1002/rem.20063.

Emmanuel, S., and B. Berkowitz. 2005. "Mixing-induced precipitation and porosity evolution in porous media." *Advances in Water Resources* 28 (4): 337-344. DOI: 10.1016/j.advwatres.2004.11.010.

Ferris, F.G., L.G. Stehmeier, A. Kantzas, and F.M. Mourits. 1996. "Bacteriogenic mineral plugging." *The Journal of Canadian Petroleum Technology* 35 (8): 56-61.

Ferris, F.G., V. Phoenix, Y. Fujita, and R.W. Smith. 2004. "Kinetics of calcite precipitation induced by ureolytic bacteria at 10 to 20 degrees C in artificial groundwater." *Geochimica et Cosmochimica Acta* 68 (8): 1701-1710. DOI: 10.1016/S0016-7037(03)00503-9.

Fetter, C.W. *Contaminant Hydrology.* (New Jersey, Prentice-Hall, Inc.) 1993.

Folkesson, A., J.A.J. Haagensen, C. Zampaloni, C. Sternberg, and S. Molin. 2008. "Biofilm induced tolerance towards antimicrobial peptides." *PLoS ONE* 3 (4). http://www.plosone.org/article/info:doi%2F10.1371%2Fjournal.pone.0001891.

Franklin, M., C. Chitnis, P. Gacesa, A. Sonesson, D. White, and D. Ohman. 1994. "*Pseudomonas aerguginosa* AlgG is a polymer level alginate C5-mannuronan epimerase." *Journal of Bacteriology* 176 (7): 1821-1830.

Fujita, Y., F.G. Ferris, F.S. Colwell, and R.W. Smith. 2000. "Accelerated calcium carbonate precipitation by aquifer organisms: A possible *in situ* remediation technique for radionuclides and metals." *American Chemical Society Annual Meeting* Washington, D.C. USA.

Fujita, Y., F. G. Ferris, R. D. Lawson, F. S. Colwell, and R. W. Smith. 2000. "Calcium carbonate precipitation by ureolytic subsurface bacteria.." *Geomicrobiology Journal* 17 (4): 305-318.

Fujita, Y., J. L. Taylor, T. L., Gresham, M. E. Delwiche, F. S. Colwell, T. L. McLing, L. M. Petzke, and R. W. Smith. 2008. "Stimulation of microbial urea hydrolysis in groundwater to enhance

calcite precipitation." *Environmental Science & Technology* 42 (8): 3025-3032. DOI: 10.1021/es702643g.

Ghiorse, W.C., and Wilson, J.T. 1988. "Microbial ecology of the terrestrial subsurface." *Advances in Applied Microbiology* 33: 107-172.

Gramling, C. M., C. F. Harvey, and L. C. Meigs. 2002. "Reactive transport in porous media: A comparison of model prediction with laboratory visualization." *Environmental Science & Technology* 36 (11): 2508-2514. DOI: 10.1021/es0157144.

Griebler, C., and T. Lueders. 2009. "Microbial biodiversity in groundwater ecosystems." *Freshwater Biology* 54 (4): 649-677.

Gruber, T., and C. Gross. 2003. "Multiple sigma sub units and the partitioning of bacterial transcription space." *Annual Review Microbiology* 57: 441-66.

Hammes, F., and W. Versraete. 2002. "Key roles of pH and calcium metabolism in microbial carbonate precipitation." *Reviews in Environmental Science and Biotechnology* 1: 3-7.

Hamon, M. 2004. "Identification of Abr-B-regulated genes involved in biofilm formation by *Bacillus subtilis*." *Molecular Microbiology* 52 (3): 847-860.

Herigstad, B., M. Hamilton, and J. Heersink. 2001. "How to optimize the drop plate method for enumerating bacteria." *Journal of Microbiological Methods* 44 (2): 121-129. DOI: 10.1016/S0167-7012(00)00241-4.

Hilgers, C., and J. Urai. 2002. "Experimental study of syntaxial vein growth during lateral fluid flow in transmitted light: First results." *Journal of Structural Geology* 24: 1029-1043.

Holmes, DE, KT Finneran, RA O'Neil, and DR Lovely. 2002. "Enrichment of members of the family *Geobacteraceae* associated with stimulation of dissimilatory metal reduction in uranium-contaminated aquifer sediments." *Applied and Environmental Microbiology* 68 (5): 2300-2306.

Janssen, D. 1981. "Nitrogen control in *Pseudomonas aeruginosa* a role for glutamate in the regulation of the synthesis of NADP dependent glutamate dehydrogenase, urease and histidase." *Archives of Microbiology* 128 (4): 398.

Janssen, D., J.A. H. Winand, , J. Marugg, and C. Van Der Drift. 1982. "Nitrogen control in *Pseudomonas aeruginosa*: mutants affected in the synthesis of glutamine synthetase, urease, and NADP-dependent glutamate dehydrogenase." *Journal of Bacteriology* 151 (1): 22-28.

Jose, S. C., M. Rahman, and O. Cirpka. 2004. "Large-scale sandbox experiment on longitudinal effective dispersion in heterogeneous porous media." *Water Resources Research* 40: 2089-2096. http://www.agu.org/journals/wr/wr0412/2004WR003363/.

Kearns, D. 2005. "A master regulator for biofilm formation by *Bacillus subtilis*." *Molecular Microbiology* 55 (3): 739-749.

Kim, J. K., S. B. Mulrooney, and R. P. Hausinger. 2006. "The UreEF fusion protein provides a soluble and functional form of the UreF urease accessory protein." *Journal of Bacteriology* 188 (24): 8413-8420.

Larrainzar, E., F. O'Gara, and J. P. Morrissey. 2005. "Applications of autofluorescent proteins for *in situ* studies in microbial ecology." *Annual Review of Microbiology* 59 (1): 257-277.

Lee, Y., and J. W. Morse. 1999. "Calcite precipitation in synthetic veins: Implications for the time and fluid volume necessary for vein filling." *Chemical Geology* 156 (1-4): 151-170. DOI:10.1016/S0009-2541(98)00183-1.

Madigan, M.T., J.M. Martinko, P.V. Dunlap, and D.P. Clark. *Brock Biology of microorganisms* (San Francisco, Pearson) 2009: 12th ed.

Meyer, F.D., S. Bang, S. Min, L.D. Stetler, and S.S. Bang. 2011. "Microbiolically induced soil stabilization: Application of *Sporosarcina pasteurii* for fugitive dust control." *American Society of Civil Engineers* Geo-Frontiers 2011: Advances in Geotechnical Engineering Proceedings of the GeoFronteirs 2011 Conference.

Mobley, H. 1995. "Molecular biology of microbial ureases." *Microbiological Reviews* 59 (3): 451-280.

Mobley, H., and R. Hausinger. 1989. "Microbial ureases: Significance, regulation, and molecular characterization." *Microbiological Reviews* 53 (1): 85-108.

Morsdorf, G, and H. Kaltwasser. 1989. "Ammonium assimilation in *Proteus vulgaris, Bacillus pasteurii,* and *Sporosarcina ureae*." *Archives of Microbiology* 152 (2): 125-31.

Neighbor, C. Honor's Thesis. Oregon State University, Department of Engineering. In preparation.

Newman, J.R., and Fuqua, C. 1999. "Broad-host-range expression vectors that carry the L-arabinose-inducible *Escherichia coli* araBAD promoter and the araC regulator." *Gene* 227 (2): 197-203.

NIH. ImageJ. *ImageJ Imaging Processing and Analysis in Java*. http://rsbweb.nih.gov/ij/.

Rahm, B., S. Chauhan, V. Holmes, T. Macbeth, L. Alvarez-Cohen, and K. Sorenson. 2006. "Molecular characterization of microbial populations at two sites with differing reductive dechlorination abilities." *Biodegradation* 17 (6): 523-534.

Roling, W., F. M, B.M. van Breukelen, M. Braster, B. Lin, and H.W. van Verseveld. 2001. "Relationships between microbial community structure and hydrochemistry in a landfill leachate-polluted aquifer." *Applied and Environmental Microbiology* 67 (10): 4619-4629.

Sar, P., S. Kazy, R. Asthana, and S. Singh. 1998. "Nickel uptake by *Pseudomonas aeruginosa*: Role of modifying factors." *Current Microbiology* 37 (5): 306-311.

Saripalli, K. P., P. D. Meyer, D. H. Bacon, and V. L. Freedman. 2001. "Changes in hydrologic properties of aquifer media due to chemical reactions: A review." *Critical Reviews in Environmental Science and Technology* 31 (4): 311-349. http://www.tandfonline.com/doi/pdf/10.1080/20016491089244.

Schultz, L. 2010. "Reactive transport in biofouled and biomineralized media". M.S. Thesis, Montana State University, Center for Biofilm Engineering.

Sharp, R.R., A.B. Cunningham, J. Kombos, and J. Billmayer. 1999. "Observation of thick biofilm accumulation and structure in porous media and corresponding hydrodynamic and mass transfer effects". *Water Science Technology* 39(7): 195-201.

Southey-Pillig, C. J., D.G. Davies, and K. Sauer. 2005. "Characterization of temporal protein production in *Pseudomonas aeruginosa* biofilms." *Journal of Bacteriology* 187 (23): 8114-8126.

Stapper, A.P., G. Narasimhan, D.E. Ohman, J. Barakat, M. Hentzer, S. Molin, A. Kharazmi, N. Høiby, and K. Mathee. 2004. "Alginate production affects *Pseudomonas aeruginosa* biofilm development and architecture, but is not essential for biofilm formation." *Journal of Medical Microbiology* 53 (7): 679-690.

Sternberg, C., B. B. Christensen, T. Johansen, A. T. Nielsen, J. B. Andersen, M. Givskov, and S. Molin. 1999. "Distribution of bacterial growth activity in flow-chamber biofilms." *Applied and Environmental Microbiology* 65 (9): 4108-4117.

Stevens, T. O, and J.P. McKinley. 1995. “Lithoautotrophic microbial ecosystems in deep basalt aquifers.” *Science* 270 (5235): 450-455.

Stewart, P. and M. Franklin 2008. “Physiological heterogeneity in biofilms.” *Nature Reviews in Microbiology* 6: 199-210.

Stoner, D. L, S. M. Watson, R. D. Stedtfeld, P. Meakin, L. K. Griffel, T. L. Tyler, L. M. Pegram, J. M. Barnes, and V. A. Deason. 2005. “Application of stereolithographic custom models for studying the impact of biofilms and mineral precipitation on fluid flow.” *Applied and Environmental Microbiology* 71 (12): 8721-8728.

Stover, C. K., X. Q. Pham, A. L. Erwin, S. D. Mizoguchi, P. Warrener, M. J. Hickey, F.S. L. Brinkman,W.W. Hufnagle, D.J. Kowalik, M. Lagou, R.L. Gaber, L. Goltry, E. Tolentino, S. Westrock-Wadman, Y. Yuan, L.L. Brody, S.N. Coulter, K.R. Folger, A. Kas, K. Lanbig, R. Lim, K. Smith, D. Spencer, G.K. Wang, Z. Wu, I.T. Paulson, J. Reizer, M.H. Saier, R.E.W. Hancock, S. Lory and M.V. Olson. 2000. “Complete genome sequence of *Pseudomonas aeruginosa* PAO1, an opportunistic pathogen.” *Nature* 406 (6799): 959-964. DOI:10.1038/35023079.

Tartakovsky, A.M., and G. Redden. 2008. “Mixing-induced precipitation: Experimental study and multiscale numerical analysis.” *Water Resources Research* (44) W06S04. http://www.agu.org/journals/wr/wr0806/2006WR005725/.

Tobin, K.J., F.S. Colwell, T.C. Onstott, and R. Smith. 2000. “Recent calcite spar in an aquifer waste plume: A possible example of contamination driven calcite precipitation.” *Chemical Geology* 169 (3-4): 449-460. DOI:10.1016/S0009-2541(00)00220-5.

United States Environmental Protection Agency (EPA)." Basics of Pump and Treat Ground Water Remediation Technology". *National Service Center for Environmental Publications (NSCEP)*. Accessed on November 21, 2011. http://nepis.epa.gov/

United States Environmental Protection Agency (EPA). "Groundwater." Report on the Environment Database. Accessed on November 21, 2011 http://cfpub.epa.gov/eroe/index.cfm?fuseaction=list.listBySubTopic&ch=47&s=201.

United States Environmental Protection Agency (EPA). "Use of Bioremediation at Superfund Sites; Fact Sheet and Order Information". *National Service Center for Environmental Publications (NSCEP)*. Accessed on November 21, 2011. http://nepis.epa.gov/

United States Geological Survey (USGS)."USGS Groundwater Information". *USGS Groundwater Information*. Accessed on November 21, 2011. http://water.usgs.gov/ogw/.

van Paassen, L.A. “Biogrout, ground improvement by microbial induced carbonate precipitation: TU Delft Institutional Repository. *TU Delft Institutional Repository* Dissertation. http://repository.tudelft.nl/view/ir/uuid%3A5f3384c4-33bd-4f2a-8641-7c665433b57b/.

van Paassen, L. A., R.Ghose, T.J.M. van der Linden, W.R.L. van der Star, and M.C.M. van Loosdrecht 2010. “Quantifying biomediated ground improvement by ureolysis: Large-scale biogrout experiment.” *Journal of Geotechnical and Geoenvironmental Engineering* 136 (12): 1721-1728.

van Paassen, L. A., C. M. Daza, M. Staal, D. Y. Sorokin, W. van der Zon, and M.C.M. van Loosdrecht. 2010. “Potential soil reinforcement by biological denitrification.” *Ecological Engineering* 36 (2): 168-175. DOI:10.1016/j.ecoleng.2009.03.026.

Wallrabenstein, C., N. Gorny, N. Springer, W. Ludwig, and B. Schink. 1995. “Pure culture of *Syntophus buswellii,* definition of its phylogenetic status, and description of *Syntrophus gentianae* sp. nov.” *Systematic and Applied Microbiology* 18 (1): 62-66.

Werner, E., F. Roe, A. Bugnicourt, M. J. Franklin, A. Heydorn, S. Molin, B. Pitts, and P.S. Stewart. 2004. “Stratified growth in *Pseudomonas aeruginosa* biofilms.” *Applied and Environmental Microbiology* 70 (10): 6188-6196.

Werth, C.J., O.A. Cirpka, and P. Grathwohl. 2006. “Enhanced mixing and reaction through flow focusing in heterogeneous porous media.” *Water Resources Research* 42. http://www.agu.org/journals/wr/wr0612/2005WR004511/.

Whiffin, V. S., L. A. van Paassen, and M. P. Harkes. 2007. “Microbial carbonate precipitation as a soil improvement technique.” *Geomicrobiology Journal* 24 (5): 417-423.

Whitman, W.B., D.C. Coleman, and W.J. Wiebe. 1998. “Prokaryotes: The unseen majority.” *Proceedings of the National Academy of Sciences of the United States of America* 95 (12): 6578-6583.

Yoon, J.H., K.C. Lee, N. Weiss, Y.H. Kho, K.H. Kang, and Y.H. Park. 2001. “*Sporosarcina aquimarina* sp. nov., a bacterium isolated from seawater in Korea, and transfer of *Bacillus globisporus* (Larkin and Stokes 1967), *Bacillus psychrophilus* (Nakamura 1984) and *Bacillus pasteurii* (Chester 1898) to the genus *Sporosarcina* as *Sporosarcina globispora* comb. nov., *Sporosarcina psychrophila* comb. nov. and *Sporosarcina pasteurii* comb. nov., and emended description of the genus Sporosarcina.” *International Journal of Systematic and Evolutionary Microbiology* 51 (3): 1079-86.

Zhang Z., S. Schwartz, L. Wagner, and M. Webb. 2000. “A greedy algorithm for aligning DNA sequences.” *Journal of Computational Biology* 7 (1-2): 203-4.

Zhang, C., K. Dehoff, N. Hess, M. Oostrom, T.W. Wietsma, A.J. Valocchi, B.W. Fouke, and C.J. Werth. 2010. “Pore-scale study of transverse mixing induced CaCO3 precipitation and permeability reduction in a model subsurface sedimentary system.” *Environmental Science & Technology* 44 (20): 7833-7838. DOI: 10.1021/es1019788.

Zhang, S., D. Li, K. Tian, Y. Bai, H. Zhang, C. Song, M. Qiao, D. Kong, and Y. Yu. 2009. “Development of a recombinant ureolytic *Lactococcus lactis* for urea removal.” *Artificial Cells, Blood Substitutes and Biotechnology* 37 (6): 227-234.

Appendix

Appendix A.

The sequence of primers used for PCR amplification of the urease operon in *E. coli* DH5α(pURE14.8) were as follows:

Forward. NNNNNN**CTGCAG**TTCATTCACATCCTACCCTAC

Bold underline is *PstI* site.

Reverse. NNNNNN**ACTAGT**CTGAGCAAAAACAAGTCAAATTAG

Bold underline is *SpeI* site.

The sequence of the urease operon in pJN105 vector and primers used for sequential sequencing are found below in figure A.1.

Figure A.1. The entire sequence of the urease insert reported in this thesis. Black with gray highlight is pJN105 promoter, black bold underlines are designed restriction sites *PstI* and *SpeI* respectively. Gray text indicates a match to the known urease sequence of DH5α(pURE14.8) *ureDABC* and *ureFG* respectively. Black text indicates newly generated sequence. Underscored sequence sections indicate primers used for the stepwise sequencing of the insert. The two blocked red nucleotides are insertions from the previously sequenced sections of DH5α(pURE14.8). They are not present when using the other basecalling software.

TCCATACCCGTTTTTTTGGGCTAGCGAATTC**CTGCAG**TTCATTCACATCCTACCCTACTTGCATTA
GCTTTTACATCACAAACACCCAATTTTGGCTGGGGTATAGCTAAACATGTTCGCGTATTTTTAGT
TGACTGAGTTGCAGGAGAAAGTATGTCTGATTTTTCAGGATCAGGCTGGTTAGCTGAAATCTTC
TTACGATATGAACTAAAACGTGGCGTCACCCGCTTAACGGATAAACAACATATCGGCCCTTTAAT
GGTTCAGCGGCCATTCTACCCCGAGCAAGGAATTGCACACACCTATTTACTTCATCCACCCGGTG
GCGTTGTCGGGGGGGATAAACTCCTTATTAATATTGATGTTCAACCACACGCCCATGCGTTATTG
ACCACGCCCGGTGCGACAAAATTTTATCGCAGTGCGGGCGGTGTTGCGCGACAAGTACAAACA
TTAACTGTTGCGCCCAATGGGTTCTTAGAATGGCTACCTCAAGAAAATATTTTTTTCCCTGAGGC

TCAAGTTCGCTTAGAAACCCACGTTCGAATCGCTAGTTCATCAAAATTTATCAGCTGGGAAATCC
AATGTTTAGGGCGCCCAGTATTAAACGAGCAATTCGACAACGGTGATATTCGGGGCCGCTTGCA
GTTTTATATTGATGACAAACTCACCTTAGCGGAATCCATATTTATCGAAGGTTCGCAAAAACAAT
CAGCCGTCATGCGTGAATTTCCTATGGTCGGCTCCTTGTATATCTACCCCGCCAGCGATGAGTTA
AAAGCTGAACTTCACGAGAGTTTGGCCGTGTTTTTCTCTACGGAAGTGAGACCGCTTGAATATG
GGCTAACTGATGTAGACGGCATTTTAGTATTACGGTTATTAGGTTCTCAAACCGAGCCGATGAT
GGCTTGCTTTGCCCATATTTGGCAGGCAACAAGACAATATTGGTTAGGTTATTGCCCAGAACCA
CCGCGTATTTGGGCAACTTAAACGTTTTTTAGGAGCAAAAAATGGAATTAACCCCAAGAGAAAA
AGATAAATTATTGCTTTTTACAGCAGGCCTCGTTGCTGAAAGGCGTTTAGCCCGTGGGCTAAAG
CTCAATTACCCTGAAGCCGTCGCGCTGATCAGTTGTGCGATTATGGAAGGCGCACGTGATGGTA
AAACTGTCGCCCAATTAATGAGCGAAGGCCGAACCCTATTAACCGCAGAGCAGGTAATGGAAG
GCGTGCCAGAAATGATCAAAGACATCCAAGTGGAATGTACATTTCCTGATGGCACAAAACTGGT
TTCTATTCACGACCCGATTGTATAGGTAACAAAATGATCCCCGGTGAAATTAAAGTCAACCACGC
TTTGGGTGATATCGAACTAAATGCAGGCCGAGAAACCCAAACGATACAAGTTGCCAACCATGGT
GACCGCCCGATTCAAATTGGCTCTCACTATCATTTTTATGAAGTCAACGACGCCCTAAAATTTGA
ACGCGAAAATACACTCGGTTTTCGTTTGAATATCCCTGCGGGCATGGCGGTACGTTTTGAACCA
GGACAAAGCCGCACAGTTGAACTTGTGGCTTTTAGCGGCAAGCGAGAAATATATGGTTTCCATG
GCAAAGTCATGGGTAAATTAGAGAGTGAGAATTAATAATGAAAACAATCTCTCGTCAAGCGTAT
GCAGATATGTTTGGTCCAACAACAGGTGACCGTTTACGCTTAGCTGATACAGAATTATTTCTAGA
GATCGAAAAAGATTTCACCACGTATGGTGAAGAGGTCAAATTTGGTGGCGGTAAAGTTATTCGT
GACGGCATGGGCCAAAGCCAAGTCACCAGTGACCTATGTGTCGATGTGCTAATCACCAACGCCA
TTATTTTAGACCATTGGGGCATTGTTAAAGCGGATATCGGGATCAAAAATGGCCGTATTGCGGG
GATTGGTAAAGCAGGTAACCCTGATGTTCAACCCAATGTCGATATCGTTATCGGCCCCGGTACC
GAAGTGGTTGCAGGCGAAGGTAAAATTATCACCGCGGGTGGCGTTGATACCCACATCCATTTTA
TTTGCCCACAGCAAGCAGAAGAAGGTCTTGTTTCCGGTGTTACCACCTTTATAGGCGGTGGAAC
TGGCCCTGTGGCTGGCACTAATGCCACTACCGTCACCCCCGGTATTTGGAATATGTACCGCATGT
TAGAAGCTGTTGATGAACTGCCTATCAACGTCGGGCTATTTGGTAAAGGCTGCGTCAGTAGGCC
CGAAGCGATTCGCGAACAAATTGAAGCGGGTGCCATTGGCTTAAAAATTCACGAGGACTGGGG
CGCTACCCCAATGGCTATTCACAACTGTTTGAATGTGGCTGATGAAATGGATGTGCAAGTGGCT
ATCCATTCAGATACGTTAAATGAAGGCGGTTTTTATGAAGAAACCGTGAAGGCCATTGCAGGAC
GAGTGATCCACGTATTCCATACAGAAGGTGCTGGCGGTGGCCATGCCCCTGACGTCATCAAATC
CGTCGGAGAACCGAATATTCTGCCTGCATCGACCAACCCAACGATGCCATACACCATCAATACC
GTTGATGAGCACTTGGATATGTTAATGGTTTGCCACCATCTCGACCCATCAATTCCAGAAGATGT
GGCTTTTGCGGAATCTCGTATTCGCCGTGAAACCATTGCTGCGGAGATATTTTGCGGAATCTCGT
ATTCGCCGTGAAACCATTGCTGCGGAAGATATTTTGCACGATATGGGCGCAATTTCTGTGATGT
CTTCAGACTCACAAGCCATGGGGCGCGTTGGTGAAGTTATCACTCGCACTTGGCAGTGCGCCCA

TAAAATGAAATTACAGCGCGGAACTTTAGAAGGTGACACACCAGAAAGCGATAATAACCGTAT
CAAACGTTATGTGGCGAAATACACCATTAACCCCGCTATCGCTCACGGTATCGCCCATGAAGTC
GGTTCGATAGAAATAGGCAAGTTAGCTGATATCGTATTATGGGACCCTGCATTTTTTGGCATCA
AACCCGCCCTAATTATGAAAGGGGGAATGGTCGCCTATGCGCCAATGGGTGATATTAACGCCG
CAATCCCAACACCACAGCCTGTACATTACCGCCCGATGTTTGGAGCATTAGGTAAAGCAAAATA
CCATACCTCAATGATTTTTATGTCAAAAGCAGGTATTGAAGCAGGTGTTCCTGAAAAATTAGGCT
TGCAGAGCCAAATAGGCCGAGTTGAAGGCTGCCGAAGCATTAGCAAAGCCTCTATGGTGCACA
ACAGTTATGTGCCACATATCGAACTTGACCCGCAAACTTATATCGTCAAAGCCGATGGTATCCCA
CTGGTATGCGAACCTGCGACTGAGTTACCGATGGCACAACGTTACTTTTTATTCTGACCCCTAAT
TAAAAGAGCCAGAGAATGAAAAAATTTATTAAAGTGGTTGCCCAACAACCCCATTCACCAAGCA
CATTAACCCTGTGCTTAACCATGGATGAGCGCACCAAAAGCCGTTTAAAAGTTACCTTAAGTGA
TGGGCAAGAAGCGGGGCTATTTTTGCCGCGCGGAACCATCCTGAAGGAAGGCGACGTTTTATC
CACTGAAGACGGTGAGTTAGTCACAATCGAAGCCGCGAAAGAGCAAGTTTCTACCGTTTACAGC
GATGACGCTCTGTTGCTCGCCCGCGTTTGCTATCACTTAGGCAACCGCCATGTTCCTTTGCAAAT
TGAAGCGGGTTGGTGCCGTTATTTTCATGACCATGTGTTAGATGATATGGCGCGTGGGTTAGGT
GCCACGGTTAGTGTCGGTTTGGAAAAATACCAACCGGAACCGGGGGCTTATGGCGGCTCATCC
GGTGGTCATCACCACCATCACGGCCACGATGATCACCATCACTAATCAGGTTCAGGGAGTGTGC
TTATGTTAGCAGATCTGCGCTTATACCAGTTAGTTAGTCCTTCTTTACCTGTTGGCTCGTTTACCT
ATTCACAAGGCTTAGAATGGGCGATTGAAAAAGGTTGGGTAACAACACCAGATACCCTTGCAG
GCTGGCTAACCGCACAAATGACGCATGCCATTGCAACATTAGAGCTTCCCGTTTTACGGCAAAT
TCAGACTTCCCTTTCCCTTGGTGATATTGAAGCGGTGAAATATTGGTGTGAATTTATGATTGCCA
GCCGTGAAACCAAAGAACTACGCCAAGAAGAGCGGCAACGAGGAATTGCTTTTGCACGATTGC
TACCTCAACTAGGCATTGAACTGGATGCTAACCTGCAAACCTGCGTGAAACAAACCCAGCTAAT
GGCCTTCGCCCTCGCCGCGGTAAATTGGCAAATTGACGTTGAAAAATTGTGCACCGCGTATGCA
TGGGGTTGGCTAGAAAACACGGTGATGTCCGGTGTTAAGCTTATCCCTTTAGGGCAAAGCGCG
GGGCAAAATATTTTATTTACCCTTGCTGAGCGCATACCCGAAGTGGTTGCGCAATCGGCAATCT
GGCCATTAGACGATATTGGTAGTTTTACACCTGCACAAATTATTGCCAGTAGTCGGCATGAAAC
CCAATACACACGACTTTTTCGTTCATGAGAAAATGCTATGCAAGAATATAATCAACCCTTAAGAA
TTGGTGTCGGTGGGCCGGTCGGCTCAGGAAAAACCGCATTATTAGAAGTGTTATGTAAAGCCA
TGCGCGACACTTACCAAATTGCCGTTGTCACCAATGATATTTACACCCAAGAAGATGCCAAAATT
TTAACCCGTGCCGAAGCACTAGATGCAGACCGCATTATTGGTGTTGAAACTGGCGGCTGCCCTC
ATACCGCTATTCGTGAAGATGCATCAATGAACTTAGCGGCCGTTGAAGAGTTAGCTATCCGCCA
TAAAAACCTTGATATCGTGTTTGTGGAAAGCGGCGGCGATAACCTCAGTGCGACGTTTAGCCCA
GAGCTGGCAGACTTAACCATTTATGTGATTGATGTTGCTGAAGGCGAAAAAATTCCACGTAAAG
GTGGGCCAGGGATCACCCATTCCGATTTACTGGTGATTAACAAAATTGACCTTGCTCCGTATGTC
GGCGCTTCATTAGAAGTGATGGAAGCCGATACCGCAAGAATGCGACCAGTAAAGCCCTATGTG

TTTACTAACTTAAAGAAAAAAGTCGGCTTAGAGACCATTATCGAGTTTATCATCGATAAAGGCAT
GTTAAGACGTTAATAAATTTGGACGCCCTATAGGTTTTATTTATAGGGCGTTTTCAATTAACAAA
TACGGGGTAAAGGCTCGCTGTGAGGCAAATCTAATAACCTTGATGTGCCGAAGATCCCAACTAA
TTTGACTTGTTTTTGCTCAGACTAGTTCTAGAGCGGCCGCCACCGCGGTGGAGCTCCAATTCGCC
CTA